

People's Democratic Republic of Algeria

وزارة التعليم العالي و البحث العلمي

Ministry of Higher Education and Scientific Research

جامعة عين تموشنت بلحاج بوشعيب

University –Ain Temouchent- Belhadj Bouchaib

Faculty of Science and Technology

Electrical Engineering Department



Final year project

Within the framework of ministerial decree 1275 «

A diploma, start-up / micro-business or patent»

To obtain a Master's degree

Branch: Electrical engineering

Specialty: Electrical Controls

Development of an innovative Aerosol Sensor based on electrical charge measurement to assess collection efficiency. (ECS)

Presented By :

1/ BOUSSAID Issam Mohamed Ali

M2

In front of a jury composed of :

Mr Walid MOHAMED

MCB U.AinTemouchent

President

Pr Massinissa AISSOU

PR U.AinTemouchent

Examiner

Dr Djillali AOUIMEUR

MAB U.AinTemouchent

Supervisor

Dr Sabah GHERBI

MCB U.AinTemouchent

Supervisor

Dr Baghdadi BENZAZZA

MCA U.AinTemouchent

Incubator representative

Pr Chahnani BOUZIANE

PR U.AinTemouchent

Head of the Center for

Technology and Innovation

Support

Academic year 2024/2025

Dedication

To my family, for their unwavering support and encouragement throughout this journey.

To my professors and mentors, whose guidance and wisdom shaped my understanding of this field.

To my friends, who offered kindness, patience, and motivation, especially during the most challenging times.

And to everyone working towards a cleaner and healthier planet—may this research on aerosol particle detection contribute to a better future.

Acknowledgment

I would like to express my deepest gratitude to all those who have supported and guided me throughout the completion of this thesis.

First and foremost, I would like to thank my supervisor, Dr Aouimer and Dr Gharbi, for their invaluable insights, constant guidance, and encouragement, which have been instrumental in shaping this research.

To my family, your constant support and faith in me have provided the strength to persevere through the most difficult moments. I am forever grateful for your love and encouragement.

Finally, to all my friends who stood by me, offering motivation, humour, and advice when I needed it most, your presence has been a source of inspiration and comfort during this journey.
Thank you all.

List of Contents:

Absract.....	6
o Introduction.....	7
o Objective.....	7
Chapter I: General Information on Electrostatic	9
Introduction.....	10
1 Filtration of Suspended Particles.....	10
I.1.1 Particulate Matter (PM) Classification.....	10
I.1.2 Air Filtration Techniques.....	11
I.2 Electrostatic Particle Precipitation.....	11
I.2.1 Operating Principle.....	11
I.2.2 Balance of Forces on a Particle.....	12
I.2.2.1 Coulomb Force.....	13
I.2.2.2 Drag Force.....	13
I.2.3 Particle Charging Mechanisms.....	14
I.2.3.1 Natural Load by Attachment.....	14
I.2.3.2 Triboelectrification.....	14
I.2.3.3 Charge by Ionic Space.....	15
I.2.3.4 Other Charging Models.....	15
I.2.4 Migration Speed of Charged Particles.....	18
I.2.5 Collection Efficiency.....	20
I.2.6 Particle Measurement and Detection.....	20
I.2.6.1 Optical Detection.....	22
I.2.6.2 Electrical Measurement.....	23
I.3 Conclusion.....	24
II.2 Chapter II: Experimental equipment and measurement methods.....	28
II.2.1 Electrostatic precipitator experimental set-up.....	28
a) Description of the powder inlet section :.....	29
b) Filtration device	29
c) Experimental equipment and instruments.....	30
II.2 New performance evaluation technique.....	33
II.2.1 ECS electrostatic aerosol sensor.....	33
II.2.2 Particle electrical charge measurement system.....	33
a- Particle feeder	34
b-Detection cell (electrical charge measurement).....	34
II.2.3 Load measurement method	35
II.2.4 Electrical charge measurement protocol.....	36
II.2.5 Experimental evaluation of electrostatic precipitator collection efficiency.....	37
II.3 Conclusion.....	38
III.1 Chapter III : Introduction	40
III.1 Assessment of collection efficiency by the classical method	40
III.2 Assessing collection efficiency by measuring electrical charge.....	42
III.2.1 ECS particle detection technique.....	42
III.2.2 Evaluation of collection efficiency using the charge difference technique ΔQ	43
III.3 Conclusion	47
IV.1 General Conclusion	49
a-Perspective.....	49
V. Bibliographical References	51

List of tables :

Table II.1: Main characteristics of the load cell.....	30
Table III.1: Efficiency as a function of tension for ESP.....	41

Table of Figures

Figure I.1: Examples of industrial air filtration systems.....	11
Figure I.2 Main stages involved in the operation of an electrostatic filter.....	12
Figure I.3 Variations in the Cunningham correction factor as a function of particle diameter	14
Figure I.4: Field lines towards the surface of an insulating particle subjected to an electric field uniform.....	15
Figure I.5 Variations in particle charge predicted by Cochet's relation as a function of particle diameter.....	17
Figure I.6: Diagram explaining the movement of a charged particle between two parallel plates.....	18
Figure I.7 Variations in relaxation time as a function of particle diameter.....	19
Figure I.8 Variations in particle charge predicted by Cochet's relation as a function of particle diameter.....	20
Figure I.9 Variations in theoretical migration velocity <i>w_{th}</i> as a function of particle size.....	20
Figure II.1: General diagram of the experimental set-up.....	26
Figure II.2: Photograph of the silica fume microparticles used.....	27
Figure II.3: Photograph of the high-voltage source.....	28
Figure II.4: Photograph of P-2132 load cell and PASCO-550 interface.....	28
Figure II.5: Photograph of the thermal propeller anemometer - Precision propeller probe.....	29
Figure II.6: Photograph of the Testo precision thermo-hygrometer.....	29
Figure II.7: Photograph of the electronic laboratory balance.....	30
Figure II.8: Photograph of the auto-transformer.....	30
Figure II.9: Photograph of the cyclone used.....	31
Figure II.10: Schematic diagram of the ECS capacitive electrostatic sensor.....	32
Figure II.11: Description of the coronacharger.....	32
Figure II.12: Description of the detection cell.....	33
Figure II.13: Load measurement schematic diagram	33
Figure II.14: Illustrative diagram of electrical charge measurement protocol	34
Figure II.15: Illustrative diagram of the protocol for evaluating the collection efficiency of an electrostatic precipitator.....	35
Figure III.1: Simultaneous variation of efficiency as a function of voltage ($Q_{ASP} = 2.1\text{m/s}$).....	39
Figure III.2: Typical diagram showing the evolution of electrical charge as a function of time for a voltage of 14 kV	40
Figure III.3: Typical diagram showing the evolution of electric charge as a function of voltage VCH for a mass of 0.5 g.....	41
Figure III.4: Load vs. time variation for ($V_{CH} = 14\text{ kV}$, $V_{ESP} = 12\text{ kV}$).....	42
Figure III.5: Load vs. time variation for ($V_{CH} = 14\text{ kV}$, $V_{ESP} = 16\text{ kV}$).....	42
Figure III.6: Load vs. time variation for ($V_{CH} = 14\text{ kV}$, $V_{ESP} = 20\text{ kV}$).....	43
Figure III.7: Comparative curves for calculating collection efficiency as a function of V_{ESP}	44

Abstract :

Introduction:

Improving the filtration efficiency of electrostatic precipitators requires an understanding of the physical phenomena involved in their operation. Numerical methods have also enabled significant progress to be made in the sizing and general architecture of any filtration system.

However, the operation of these filters is not always stable, and fluctuations in filtration efficiency frequently occur, necessitating the implementation of a monitoring system and permanent quantification of discharge concentrations [1-2]. Consequently, the detection, sampling and counting of these particles using precise instruments are of paramount importance in preserving air quality [3]. Most of these instruments, currently indispensable to any filtration process, operate intermittently and can only analyze a puncture of the total polluted flow.

Objective:

The detection and measurement of airborne solid or liquid aerosol particles with aerodynamic diameters between 1 nm and 100 μm has become an important topic in air pollution monitoring and source characterization. In recent years, there has been considerable interest in submicron aerosol particles, defined as suspended aerosol particles with aerodynamic diameters of less than 2.5 μm , for two main reasons. Firstly, these particles have been associated with adverse health effects in areas of high concentration, and secondly, aerosols are believed to have a significant influence on atmospheric quality, local and global climate and processes in various industries such as food, pharmaceutical and medical, electronics and semiconductor [4]. To this end, aerosol particle instruments have been developed to monitor indoor and outdoor aerosols in the pollution and process control industries [5-6].

A number of commercial instruments are available, using various methods to detect and measure the size distribution and number or mass concentration of particles. Available instruments include a Palas Model Welas-1000 granulometer based on the use of a white light source [7], a Scanning Mobility Particle Analyzer (SMPS) using the electrical mobility of particles [8], a condensation particle counter (CPC) using particle growth and optical properties [9-10], an electrical aerosol detector (EAD) using the electrostatic charge measurement technique [11] and an electrical low-pressure impactor (ELPI) using particle inertial impact under low pressure [12]. These commercial instruments are widely used

to measure airborne ultrafine particles and provide high-resolution measurements, but they are very expensive and large in size.

The present manuscript is structured around three chapters. In the first chapter, we present a literature review on electrostatic precipitation as an air pollution control tool and the applications of discharges for particle charging and collection, taking care to recall pollution vectors and air pollution control techniques, before going into detail on what electrostatic precipitation encompasses by reviewing the processes involved upstream, during and downstream of the phenomenon.

The second chapter focuses on the detailed description and definition of the characteristics of the various device components, as well as the measurement protocols and techniques used for the different experimental rigs.

Finally, the third chapter looks at a new aerosol presence detection system that detects particles suspended inside a capacitive electrostatic sensor (ECS) connected to a sensitive electrometer, in order to assess the collection efficiency of precipitators.

We conclude with some conclusions and prospects.

CHAPTER I :

General Information On Electrostatic Precipitators

Introduction :

In the first chapter, we present an overview of the literature on electrostatic precipitation as an air pollution control tool and the applications of discharges for charging and collecting particles, taking care to recall pollution vectors and air pollution control techniques, before going into detail on what electrostatic precipitation encompasses by reviewing the processes involved upstream, during and downstream of the phenomenon.

I.1 Filtration of suspended particles

Airborne particles, or aerosols, are made up of solid and/or liquid substances with a fall velocity that is usually negligible. The presence of airborne particles is mainly due to atmospheric pollution.

Atmospheric pollution is caused by the direct or indirect introduction by man of substances into the atmosphere and enclosed spaces, with harmful consequences such as endangering human health, damaging biological resources and ecosystems, influencing climate change, damaging material assets and causing excessive olfactory nuisance [13].

Aerosols are primary pollutants, defined as substances present in the atmosphere as they are emitted. Particle size is the most important parameter for characterizing aerosol behavior. There are almost all shapes and sizes of particles, depending on their nature and whether they originate from aggregates of solid or liquid matter suspended in the air [4].

In metrology, a distinction is made according to particle size: "PM₁₀" (Particulate Matter), "PM_{2.5}", "PM₁" or "PM_{0.1}". PM₁₀ are particles with an average diameter of less than 10 μm. Whereas PM_{2.5}, PM₁ and PM_{0.1} are particles whose diameter does not exceed 2.5 μm (called fine particles), 1 μm (very fine particles) and 0.1 μm (ultrafine particles or nanoparticles) respectively. It is important to note that particles with an aerodynamic diameter greater than 10 μm are retained by the upper airways (nose, mouth). PM₁₀ are so-called "respirable" particles and include fine, very fine and ultrafine particles, and can therefore penetrate the bronchial tubes. PM_{2.5} includes very fine and ultrafine particles and penetrates the pulmonary alveoli. And finally, PM₁ includes ultrafine particles and can pass the alveolar-capillary barrier [14-16].

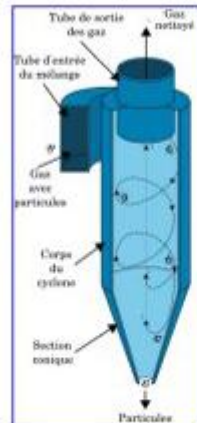
Particulate matter or dust is no ordinary pollutant. Whereas for all other substances, it's enough to measure the weight of emissions to get an accurate idea of how air quality is evolving, for particles the problem is more complex. Their toxicity is not directly related to their weight.

On the contrary the finest particles are generally considered the most dangerous, due to the difficulty of trapping them through filters, their ability to penetrate deeper into the respiratory tract and their longer suspension time in the air.

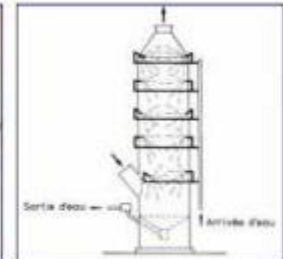
Numerous air filtration techniques have been developed in response to the growing problem of air pollution, particularly in the industrial sector. These devices fall into four categories (Figure I.1):

- mechanical filters
- hydraulic filters

- layer filters
- electric filters or electrostatic precipitators



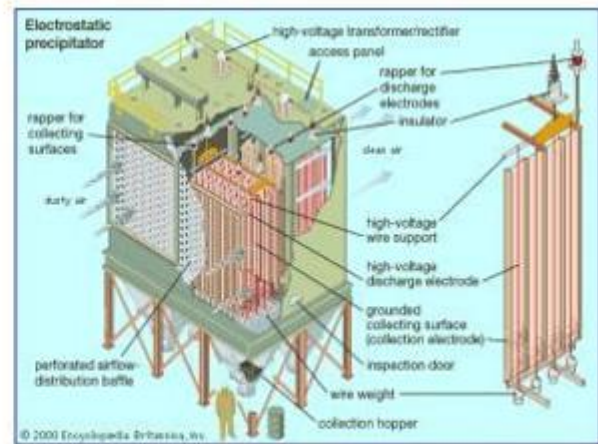
(a) mechanical filters



(b) hydraulic filters



(b) layer filters



(b) electric filters or electrostatic precipitators

Figure I.1: Examples of industrial air filtration systems[17]

I.2 Electrostatic particle precipitation

I.2.1 Operating principle

The electrostatic filter is a device in which electrostatic forces trap particles contained in a gas. It consists of a set of active and passive electrodes.

collection electrodes and can be either flat or cylindrical in geometry. The discharge generated within this device, often maintained at a high negative potential, produces ions by the attachment of free electrons to gas molecules. When these ions collide with particles, the latter become charged, then move towards the collecting electrodes in the direction of the electric field. This process is known as electrostatic precipitation [18-20].

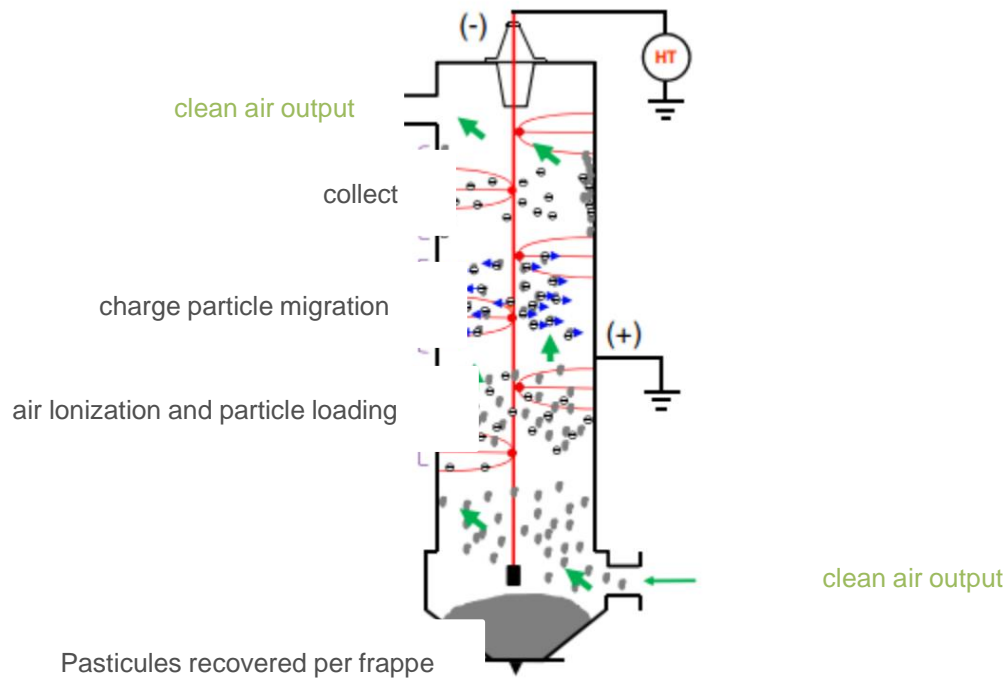


Figure I. 2 Main stages involved in the operation of an electrostatic filter [21].

To explain the operating principle of an electrostatic precipitator, let's take the example of an industrial electrostatic precipitator with a cylindrical geometry (Figure I.2). It consists of a vertically arranged metal cylinder (the collection electrode) and a wire suspended along the cylinder's central axis (the active electrode). The active electrode is connected to high-voltage DC, while the collection electrode is connected to ground.

When a voltage is applied above a threshold (discharge ignition voltage), a corona discharge appears around the wire. It appears either as luminous spots (negative DC voltage) distributed along the wire and called "*Tufts*", or as a "luminous sheath" (positive DC voltage). The luminous phenomena locally represent the ionized regions of the gas from which ions of the same polarity as the active electrode are emitted towards the collection electrode. These ions pass through the inter-electrode gap under the action of a DC electric field, towards the collection electrode. When polluted gases are introduced through the lower part of the electrostatic precipitator, they pass upwards through the inter-electrode space. The particles they contain pick up ions and become strongly charged; they are then subjected to the Coulomb force, which directs them towards the inner surface of the electrostatic precipitator, where they are deposited [18-20].

The gases leave the electrostatic precipitator through the upper part, while the trapped particles accumulate on its inner surface, forming a layer of dust. By mechanically striking the walls of the electrostatic precipitator with a hammer, the dust falls to the bottom of the electrostatic precipitator, where it is removed by means of a special device.

I.2.2 Balance of forces on a particle

In an electrofilter, particles can be subjected to the following forces: drag (mean force + stochastic components related to Brownian motion and turbulence), centrifugal and gravitational forces (neglected here), electrostatic forces (image forces, Coulomb force, dipole force) and Van der Waals forces as they approach a substrate.

In most cases of particle trajectory resolution, only Coulomb forces [22-23] and drag forces are taken into account. Indeed, gravitational forces can be considered negligible for submicron particles, given the time scales observed in electrostatic precipitators (at most a few seconds residence time). Furthermore, short-range forces such as the Van der Waals force, the image force and the dipole force are very weak and have very little influence on the trajectory of particles in the inter-electrode space, which is infinitely larger than the order of magnitude of the range of these forces [24].

In this section, we'll just mention the two forces involved: the Coulomb force and the drag force.

1.2.2.1 Coulomb force

A charged particle is subject to an electrostatic force as soon as it is relatively close to charged surfaces or other charged particles. In the presence of an electric field \vec{E} , particles that have acquired an electric charge q_p experience the force of Coulomb \vec{F}_e proportional to the load, whose expression is :

$$\vec{F}_e = q_p \vec{E}$$

Expression (I.1) is the basic equation for the electrostatic force acting on particles suspended in electrostatic filters.

1.2.2.2 Drag force

The drag force is given by the following relationship [20] :

$$\vec{F}_f = \frac{1}{2} C_f (Re_p) \cdot S_p \cdot \rho_g \cdot V_{rel} \cdot \vec{V}_{rel}$$

In relation (I.2), S_p represents the cross-sectional area of the particle (the cross-sectional area of the particle intercepted by the fluid), ρ_g is the density of the carrier gas, \vec{V}_{rel} is the relative velocity of the particle with respect to the gas and $C_f (Re_p)$ is the drag coefficient.

The drag coefficient depends on the particle's Reynolds number Re_p , which represents the ratio between inertial forces and viscous effects [25]:

$$Re_p = \frac{d_p \cdot |\vec{V}_{rel}|}{\nu_g} = \frac{d_p \cdot |\vec{U}_g - \vec{w}|}{\nu_g}$$

Where ν_g is the kinematic viscosity of the gas (at atmospheric pressure and temperature ambient $\nu_g = 1.55 \times 10^{-5} \text{ m}^2/\text{s}$), d_p is the particle diameter, \vec{U}_g is the speed of

the flow and \vec{w} the particle velocity. If $Re_p \ll 1$, a condition met in the case of electrostatic

precipitators [18, 20], when particles have a diameter of less than 20 μm , the drag coefficient has the following expression:

$$C_f = \frac{24}{Re_p}$$

In this situation, the frictional force between a spherical particle and the gas is given by Stokes' relation [20] :

$$\vec{F}_f = 3\pi \cdot n_g \cdot d_p \cdot (\vec{U}_g - \vec{w}) \cdot \frac{1}{Cu(d_p \cdot \lambda_g)} \quad (I.5)$$

Where \vec{U}_g is the dynamic viscosity of the gas. If the size of the particle is comparable to the mean free path λ_g of the gas molecules, the particles will move within a discontinuous medium. In this case, equation (I.5) must be corrected by the Cunningham factor [19] :

$$Cu = 1,257 \frac{2\lambda_g}{d_p} + 0,4 \frac{2\lambda_g}{d_p} \exp\left(-1,1 \frac{d_p}{2\lambda_g}\right)$$

The mean free path of the gas molecules is given by the relationship:

$$\lambda_g = 6,61 \times 10^{-8} \left(\frac{T}{293}\right) \left(\frac{101,3 \times 10^3}{P}\right)$$

Figure I.3 shows the variation of the Cunningham factor as a function of particle diameter in the case of air at atmospheric pressure and ambient temperature $\lambda_g = 66.1 \text{ nm}$.

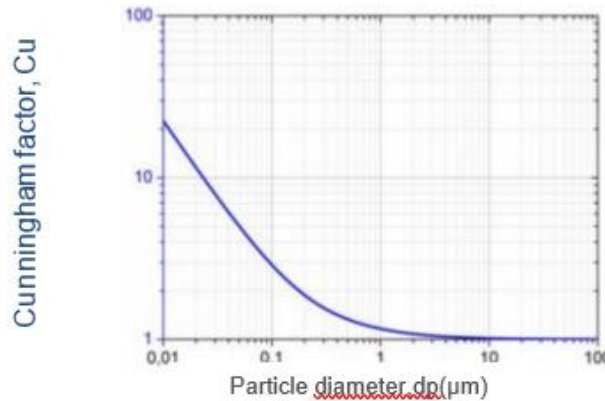


Figure I. 3 Variations in the Cunningham correction factor as a function of particle diameter ($\lambda_g = 66.1 \text{ n}$)

I.2.3 Particle charging mechanisms

The various particle charging mechanisms and their saturation charge are widely studied phenomena, and many authors have come up with relatively realistic solutions for spherical particles.

In this section, we present the main particle charging mechanisms, with particular emphasis on the ionic space charge mechanism.

I.2.3.1 Natural load by attachment

In the earth's atmosphere, positive and negative ions are continuously generated by the action of cosmic radiation and radioactive gases emanating from the ground. As

presented by Hinds [4], air contains around 1000 ions/cm³ with, to a first approximation, an equal number of positive and negative ions. Aerosol particles, which are initially neutral, can acquire a charge by collision (due to their random thermal motion) with ions. However, charged particles tend to lose their charge slowly, attracting ions of opposite sign.

I.2.3.2 Triboelectrification

Triboelectrification covers two causes of electrification: friction and contact [26-27]. In frictional charging, i.e. when two different particles rub against each other, there is a transfer of charge (mainly electrons) from the surface of one particle to that of the other. This process uses the difference in electronic structure of the two surfaces, with one particle becoming positively charged and the other negatively charged. This phenomenon means that in clouds of particles carried by an air stream, a high proportion of particles are charged by contact with the walls or by collisions.

Contact charging occurs during the separation of dry, non-conducting particles from solid surfaces [4, 28]. In this process, when a particle touches a surface, charges are transferred, so that the particle acquires a net positive or negative charge when it separates from the surface. The polarity of the charged particle and the number of charges on it depend on the materials and their relative positions in the triboelectric series. Friction increases the number of charges acquired. Because it requires dry surfaces, contact charging becomes ineffective in conditions of relative humidity greater than around 65%.

I.2.3.3 Charge per charge of ionic space

The various mechanisms of particle charging and saturation charging are widely studied phenomena, and many authors have come up with relatively realistic solutions for spherical particles. In this section, we present the main particle charging mechanisms, with particular emphasis on the ionic space charge mechanism.

The main cause of particle motion in electrostatic filters is the Coulomb force. This varies linearly with particle charge. Consequently, an increase in particle charge is required to ensure migration towards the precipitator's collecting electrodes [29]. This can be brought about by a high density of space charges produced by an electrical discharge in the inter-electrode gap. This discharge mechanism will be described later. The particle charging process then depends on several factors, the most important of which are ionic charge density, local electric field strength and particle size [24, 29, 30]. Numerous studies [20, 4, 31] have shown that the charging process can be attributed mainly to the following mechanisms: field charging, diffusion charging and mixed charging.

a. **Load per field :**

As the name suggests, in this charging mechanism, ions are brought to the particle surface by the electrostatic force caused by an external electric field [29-30]. This force is balanced by the repulsive force created by the charge distributed on the particle's surface. Indeed, a particle in a gas causes local distortion of the electric field, with the field lines ending up at the particle's surface. This field distortion depends on the nature of the particle: when the particle is conductive, the field distortion is maximal [29-30].

For an insulating (non-conducting) particle, the field distortion depends on its permittivity. As a result, the electric field intensity increases at the surface of the particle. In this case, ions present in the gas and moving along the field lines can reach the particle surface [29-30]. Each ion that reaches the particle surface alters the local electric field distribution. However, as long as the electric field created by the particle's charge is less than

the maximum field that exists at the particle's surface when it is uncharged, the ions continue to reach the particle's surface [29-30]. When sufficient charge has been acquired, the field lines bypass the particle.

The particle is said to have acquired the "field saturation charge" noted q_{ps} (Figure I.4).

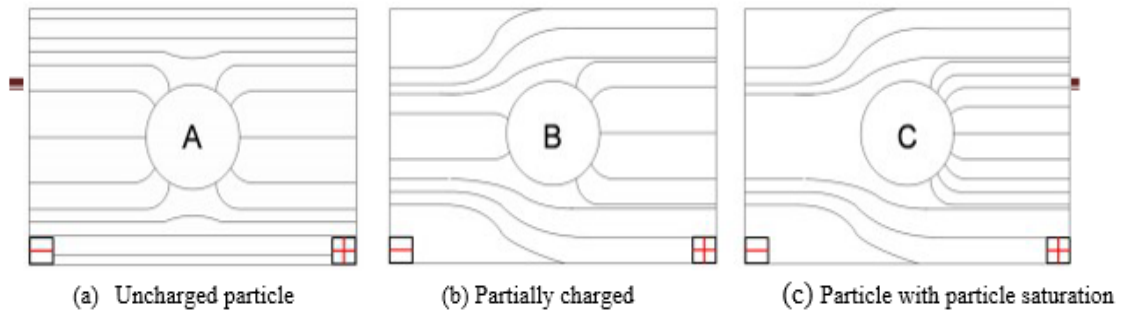


Figure I. 4: Field lines towards the surface of an insulating particle subjected to an electric field uniform [4,32]

Rohmann first developed a theory of field charging in 1923 [33], completed by Pauthenier in 1932 [34-35]. These authors show that ions arrive at the surface of a particle as long as the particle's charge is not sufficient to repel them. Pauthenier showed that, due to the phenomenon of electrostatic repulsion, only a small part of the particle surface is reached by ions. Other authors have made contributions along the same lines [36-38]. The charge of a spherical particle is given by Pauthenier's field charge equation [35] :

$$q_p(t) = q_p^s \frac{t}{t + \tau}$$

With

$$q_p^s = \pi \cdot \epsilon_0 \cdot \frac{3\epsilon_r}{\epsilon_r + 2} \cdot d_p^2 \cdot E$$

And

$$\tau = 4 \cdot \frac{\epsilon_0}{\rho_i \cdot \mu_i} = 4 \cdot \frac{\epsilon_0}{e \cdot n_i \cdot \mu_i} = 4 \cdot \frac{\epsilon_0 E}{J}$$

Where q_p^s is the saturation charge (C), t the charging time (s), τ the charging time constant per field (s), ϵ_0 the permittivity of vacuum ($\approx 8.85 \times 10^{-12} F/m$), ϵ_r the relative

permittivity of the material making up the particle, d_p the particle diameter (m), E the electric field (V/m), J the current density (A/m²), ρ the charge density (C/m³), μ the ionic

mobility ($m^2 /V.s$), e the electronic charge ($\approx 1.602 \times 10^{-19} C$) and n_i the ion concentration in space (m^{-3}). For a conducting particle $\epsilon_r \rightarrow \infty$, equation 1.9 becomes :

$$q_p^s = 3\pi \cdot \epsilon_0 \cdot d_p^2 \cdot E$$

For large particles ($d_p \geq 1\mu m$), the field-charge mechanism is dominant. For small particles ($d_p \leq 0.1 \mu m$), thermal diffusion becomes dominant and diffusional charging becomes important [35, 39- 41].

b. Diffusion load :

In a cloud of ions and in the absence of an electric field, particles are charged by Brownian motion between ions and particles: this mechanism is called diffusion charging and does not require an external electric field [30]. This mechanism involves the probability of collision between particles and ions animated by random thermal agitation [29]. Under these conditions, all the surface elements of a particle have the same probability of collision with the ions, and the particle can accumulate a certain electrical charge [29-30]. This diffusion charging mechanism is of greater importance for very fine particles, with a diameter of less than $0.1 \mu m$ [18, 20]. In diffusion charging, the amount of charge accumulated depends on particle size, ion density, average ion thermal agitation velocity, particle dielectric constant, absolute gas temperature, and particle residence time within the field. Several models of the diffusion charging mechanism have been developed in the literature [42-44]. The expression for diffusion charging

$q_p(t)$ of a particle given by White [44] is:

$$q_p(t) = q^* \ln \left(1 + \frac{t}{\tau^*} \right)$$

With

$$q^* = 2\pi \cdot \epsilon_0 \cdot d_p \cdot \frac{k_B \cdot T}{e}$$

And

$$\tau^* = \frac{8 \cdot \epsilon_0 k_B \cdot T}{d_p \cdot C_i \cdot n_i \cdot e^2} = 8\epsilon_0 \sqrt{\frac{m_i \cdot k_B \cdot T}{3}} \cdot \frac{\mu_i \cdot E}{d_p \cdot J \cdot e} \quad (l. 14)$$

Where q^* is the charge constant (C), τ^* the diffusion charge time constant (s), k_B the Boltzmann constant ($\approx 1.38 \times 10^{-23} J/K$), T the temperature (K), e the electronic charge ($\approx 1.602 \times 10^{-19} C$), C_i the thermal velocity of the ion (m/s), n_i the concentration of ions in space (m^{-3}), m_i the mass of an ion (kg) and μ_i the mobility of an ion ($m^2 /V.s$).

c. Mixed load :

Both mechanisms operate simultaneously for particles between 0.1 and $1 \mu m$ in size [41]. However, the total charge acquired by a particle at the end of the process is not the sum of the charges contributed by each of the two mechanisms. A number of studies have been carried out on mixed charging, in particular by Lawless and Altman [45-47], who modified pre-existing models and came up with fairly simple relationships between the two mechanisms.

which take into account the interactions of the two loading mechanisms. Smith and McDonald [48] have also developed a formula that combines the two loading mechanisms. In this section, we will focus on the loading theory given by Cochet [49], as this is the one we will use in our model.

When the mean free path of the ions becomes of the same order of magnitude as that of the particles, it can be assumed that all ions entrained inside the pressure tube whose envelope passes at a distance equal to the mean free path of the ions and whose center is that of the particle are captured [24]. Cochet therefore proposes a combined relationship for calculating the limiting charge of a particle by field effect and by diffusion towards its surface. The saturation charge of a particle of diameter d_p is given by the relation :

$$q_p^s = \left[\left(1 + \frac{2\lambda_g}{d_p} \right)^2 + \left(\frac{2}{1 + \frac{2\lambda_g}{d_p}} \right) \cdot \left(\frac{\epsilon_r - 1}{\epsilon_r + 2} \right) \right] \cdot \pi \cdot \epsilon_0 \cdot d_p^2 \cdot E$$

Where ϵ_0 the permittivity of vacuum and ϵ_r the relative permittivity of particles.

This relationship is currently the most widely used, as it covers the boundary charge of particles over a very wide range of sizes and operating conditions [24]. Figure I.5 shows the variation of the limiting charge as a function of particle diameter, considering two values of the electric field strength E .

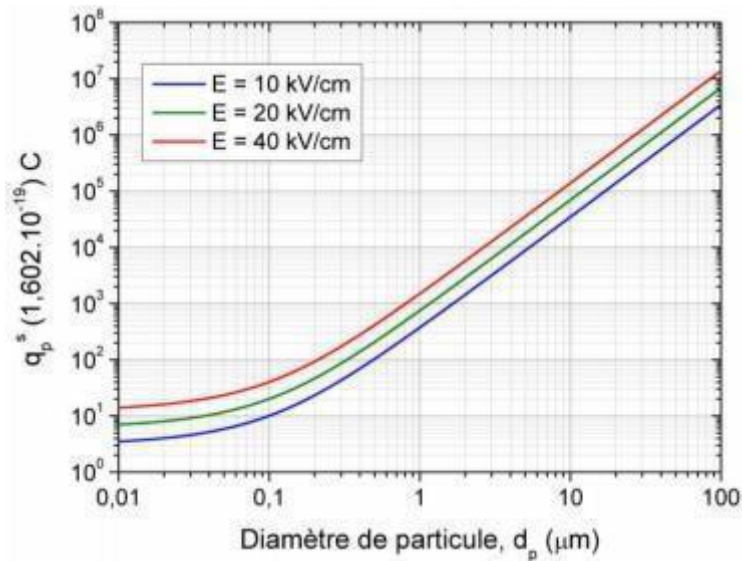


Figure I. 5 Variations in particle charge predicted by Cochet's relation as a function of particle diameter

$$(T=293K, \lambda_g=66.1 \text{ nm}, \epsilon_r=4)$$

I.2.3.4 Other load models

In the literature, other particle loading models have been developed. They are based on the Knudsen number, generally noted K_n , which is an adimensional number enabling the flow regime to be determined in terms of the continuity of the medium, rather than in terms of the flow rate.

turbulence terms of a fluid. It is defined as the ratio of the mean free path λ to the particle radius r_p [50] :

$$K_n = \frac{\lambda}{r_p}$$

Depending on the Knudsen number K_n , three flow regimes can be distinguished: Free molecule regime ($K_n \gg 10$), transition regime ($0.1 \leq K_n \leq 10$) and continuous regime ($K_n \leq 0.1$).

This shows that for large particles immersed in a strong electric field, charging by field effect is predominant, whereas for small particles immersed in a weak field, charging by diffusion is predominant [51]. The two charging mechanisms work together to provide particles with an overall charge, the relative importance of which is mainly determined by their size and the intensity of the electric field.

The particles inside an electrostatic precipitator, once charged by these various mechanisms, experience Coulomb force when subjected to an electric field. This electrostatic force is responsible for their movement towards the collecting electrodes. It is this process, known as "migration", that we will now study.

I.2.4 Migration speed of charged particles

Let be a spherical solid particle of diameter d_p , electric charge q_p and velocity \vec{w} located in a laminar gas flow of velocity \vec{U}_g , subjected to an assumed uniform and constant electric field \vec{E} (figure I.6). Its motion inside the precipitator is governed by the fundamental relation of dynamics :

$$m_p \cdot \frac{d\vec{w}}{dt} = \vec{F}_e + \vec{F}_f$$

Where m_p represents the mass of the particle, \vec{F}_e and \vec{F}_f respectively the electrical force and particle, the drag force.

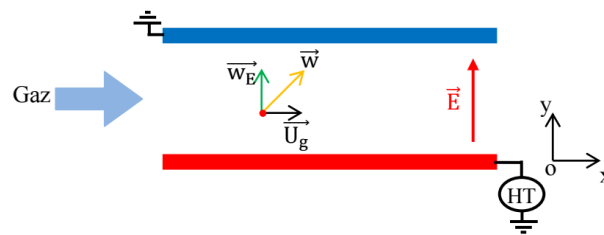


Figure I. 6: Diagram explaining the movement of a charged particle between two parallel plates.

By replacing the expression of each force in relation I.17, the migration of the particle towards the collection electrode along the Oy axis is characterized by the solution of the

following differential equation:

$$\frac{dw_E}{dt} + \frac{3\pi \cdot \eta_g \cdot d_p}{m_p \cdot Cu} \cdot w_E = \frac{q_p}{m_p} \cdot E$$

Where w_E is the component of a particle's velocity in the direction normal to the plates, known as the "effective migration velocity". If we consider that at the initial time

$t = 0$, the particle's velocity w_E is zero, the solution of equation I.18 gives the following evolution over time:

$$w_E(t) = w_{th} \left[1 - \exp \left(-\frac{t}{\tau_p} \right) \right]$$

Where is called theoretical migration speed [18, 20, 52] and is expressed as :

$$w_{th} = \frac{q_p \cdot E}{3\pi \cdot \eta_g \cdot d_p} C u$$

In relation I.19, τ_p is the relaxation time of the particle considered, which depends on the mass and size of the particle, as well as the dynamic viscosity of the carrier gas:

$$\tau_p = \frac{m_p}{3\pi \cdot \eta_g \cdot d_p} \cdot C u = \frac{\rho_p \cdot d_p^2}{18 \cdot \eta_g} \cdot C u$$

Where ρ_p is the particle density. The time τ_p characterizes the particle's transient behavior until it moves at constant velocity w_{th} . Note that the relaxation time is independent of the electrical conditions inside the filter. Figure I.7 shows variations in τ_p as a function of particle diameter. Note that for fine particles ($d_p \leq 1 \mu m$), this time is very small ($\tau_p \leq 10 \mu s$).

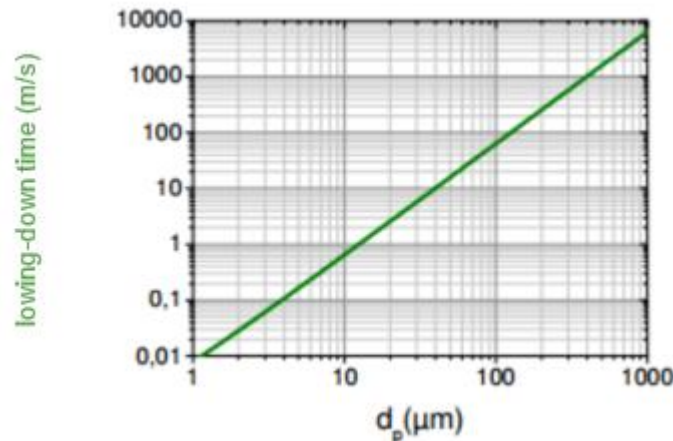


Figure I. 7 Variations in relaxation time as a function of particle diameter

$$(T=150^\circ C, \eta_g=2.37 \times 10^{-4} \text{ kg/m} \cdot \text{s}, \rho_p = 2700 \text{ kg/m}^3)$$

In this approach, the theoretical migration velocity (relation I.20) represents the stationary value of the particle velocity in the direction of the electric field (perpendicular to the collector plates), and characterizes the particle migration process inside the electrofilter. All analytical models are based on this concept.

A study of the theoretical migration velocity requires knowledge of the electrical charge of particles as a function of their size. To show the variation of w_{th} as a function of particle

size, a simple charge calculation relationship established by Cochet [49] is generally used. This relation gives the limiting charge per field of a particle that is in an electric field of

strength E . It offers a good

correlation with experimental results for $d_p > 0.3 \mu m$ [49] :

$$q_p^s = \left[\left(1 + \frac{2\lambda_g}{d_p} \right)^2 + \left(\frac{2}{1 + 2\lambda_g/d_p} \right) \cdot \left(\frac{\epsilon_r - 1}{\epsilon_r + 2} \right) \right] \cdot \pi \cdot \epsilon_0 \cdot d_p^2 \cdot E$$

Where ϵ_0 is the permittivity of vacuum and ϵ_r is the relative permittivity of particles.

Figure I.8 shows the variation of the boundary charge as a function of particle diameter, considering two values of the electric field intensity E .

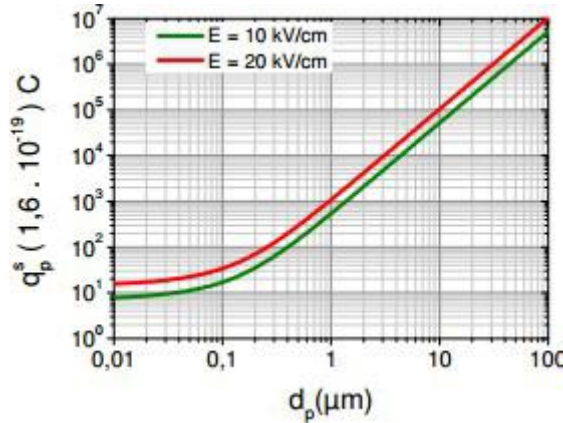


Figure I. 8 Variations in particle charge predicted by Cochet's relation as a function of particle diameter

($T = 150^\circ\text{C}$, $\lambda_g = 0.101 \mu\text{m}$ et $\epsilon_r \rightarrow \infty$, case of conductive particles).

Using the results of Figure I.8 on the electric charge of the particles, we can evaluate the values of the theoretical velocity w_{th} (Figure I.9). The variation of the velocity w_{th} as a function of particle diameter passes through a minimum value for $w_{th} \cong 0.25 \mu\text{m}$.

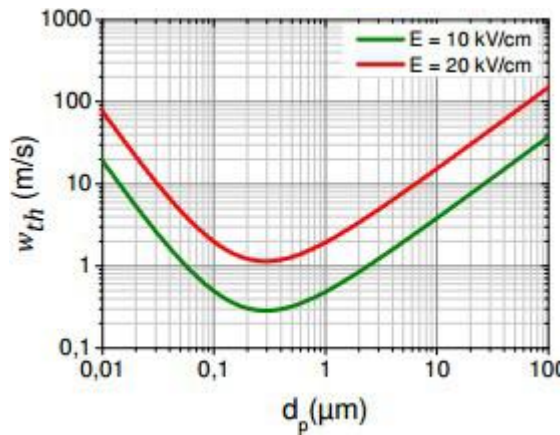


Figure I. 9 Variations in theoretical migration velocity w_{th} as a function of particle size

($T = 150^\circ\text{C}$, $\lambda_g = 0.101 \mu\text{m}$, $U_g = 2.37 \times 10^{-5} \text{ kg/m. s}$).

A low migration speed reduces particle transport to the collector plates, and consequently collection efficiency. So, as particle migration velocity is at its lowest for particle sizes between 0.1 and $1 \mu\text{m}$, so is collection efficiency.

1.2.5 Collection efficiency

As with any electrical device, we need to estimate the efficiency of an electrofilter in order to assess its effectiveness. To express the efficiency of a filter with respect to a given aerosol, we consider three quantities: the amount of aerosol upstream of the filter (q_{am}), the

amount of aerosol downstream of the filter q_{av} and the amount of aerosol retained by the filter ($q_{am} - q_{av}$). From these three quantities, we can express three ratios:

- The efficiency n_E which is the ratio of the quantity of aerosols retained by the filter to the quantity of aerosols upstream:

$$n_E(\%) = \frac{q_{am} - q_{av}}{q_{am}} \cdot 100$$

The permeance P_E is the ratio of the quantity of aerosols downstream to the quantity of aerosols upstream.

Aerosols upstream :

$$P_E(\%) = \frac{q_{av}}{q_{am}} \cdot 100$$

The purification coefficient C_E is the ratio of the quantity of aerosols upstream to the quantity of aerosols downstream.

Quantity of downstream aerosols :

$$C_E(\%) = \frac{q_{am}}{q_{av}} \cdot 100$$

There are a number of different methods for measuring filter efficiency, each of which has its own characteristics.

characterized by a test aerosol and by the method used to measure aerosol quantities. The European Association of Aircraft Manufacturers (EUROVENT), followed by the International

Organization for Standardization (ISO), have standardized some of the most common aerosol test methods.

We distinguish three main families of measurement methods. The first two include filters known as general ventilation filters, with one family for medium-efficiency filters and another for high-efficiency filters; the third family of filters, known as ultra-high-efficiency filters, capture submicron particles.

The overall collection efficiency n_t of any gas treatment system, regardless of its type, can be determined using the following formula:

$$n_t = 1 - \frac{n_s}{n_e} \cdot 100 \quad 26$$

Where n_e and n_s represent, respectively, the overall concentration of particles at the filter inlet and outlet. Collection efficiency can also be determined from particle number and mass.

In view of the very diverse particle size distribution, it may be interesting to express collection efficiency in terms of particle size classes. With each class corresponding to an average diameter d_p , this efficiency, known as fractional efficiency, is defined by the following relationship for particle size class i :

$$n_f^i = 1 - \frac{m_s(d_p^i)}{m_e(d_p^i)} = 1 - \frac{C_s(d_p^i)}{C_e(d_p^i)} \quad 27$$

Where $m_e(d_p^i)$ and $m_s(d_p^i)$ are the masses of particles of class i at input and output of the precipitator. Fractional efficiency can also be expressed in terms of concentrations, in expression I.27, $C_e(d_p^i)$ and $C_s(d_p^i)$ being the average concentrations

of class i particles at the filter inlet and outlet. When the collection efficiency is close to unity, the performance of a precipitator can be best characterized by the penetration Pn_t which is expressed as follows:

$$Pn_t = 1 - n_t = 1 - \frac{n_s}{n_e} \quad 28$$

Thus, using penetration to represent the performance of an electrostatic precipitator enables us to better follow its variations when said performance peaks at over 99%. That said, the performance of an electrostatic precipitator depends on its type. There are different types of electrostatic precipitator, depending on the application for which they are intended. They are classified as cylindrical or planar (shape of collection electrodes), vertical or horizontal (direction of effluent gas), single-stage or two-stage (electrode geometry) and dry or wet (with or without the use of liquid).

1.2.6 Particle measurement and detection

There are two main techniques for measuring and detecting particles in mobility analyzers: (a) optical, and (b) electrical. The following paragraphs give a brief description of these two methods.

I.2.6.1 Optical detection

Measuring the scattering and absorption of light by aerosol particles is another method for

detecting and assessing their number concentration. When aerosol particles are exposed to light, the scattering and absorption of part of the light and the resulting reduction in light intensity are described by the Lambert-Beer law. The scattering of light by particles depends on their size relative to the wavelength of the light, and the phenomena are described by different theories. For particles whose diameter is less than around 50 nm, Rayleigh theory is applied, while for particles whose size is between 50 nm and 100 μm , Mie theory is used to estimate the intensity of scattered visible light. In the size range where the particle size and the wavelength of the light used are of the same order, light scattering by aerosol particles is a complicated phenomenon. According to Rayleigh's and Mie's theories, the intensity of scattered light is proportional to the sixth power of the particle diameter, indicating a rapid increase in scattered light intensity as a function of particle size; the theories also show that ultrafine particles are very difficult to detect by light scattering techniques, since the intensity of scattered light is very low [4].

There are two types of optical detectors: single particle counters, which measure the light scattering and light extinction of individual particles, and photometric counters, which measure the same phenomena but for a set of particles (multiple particle counters). Optical single-particle counters can measure aerosols at very low concentrations. In principle, a beam of aerosol is directed through a condensed light beam. The light scattered by each particle is received by a photodetector and converted into an electrical signal. Particle number concentration is determined by the number of pulses produced by the sensor, while an indication of particle size can be obtained from the amplitude of the output signal each time. The first particle detector Optical counters use white light to detect particles, while modern counters use laser sources.

Multi-particle optical instruments are commonly used to measure aerosols with high particle concentrations. Installation of these instruments is much simpler than that of simple optical particle counters. The aerosol stream is drawn through a light beam and the total scattering of each particle in the stream is measured by a light intensity sensor, and the readings are then related to particle number concentrations. An important parameter of this type of counter is the type of gas in which the particles are suspended, as this would contribute to the

This would result in regular noise in the output pulse. To avoid this signal noise, air is usually replaced by a gas with known diffusion properties.

For the sub-micrometer size range, the particle detection efficiency of optical methods is reduced, necessitating particle growth techniques. The most common growth method used in these instruments is the condensation of supersaturated gaseous species onto particles. Such devices (CPC condensation particle counters) are widely used for particle counting in many aerosol measurement instruments.

The main advantage of instruments that rely on optical methods to detect and measure aerosols is that they respond quickly and do not require physical contact with the particles.

I.2.6.2 Electrical measurement :

Electrical particle measurements have been widely used in aerosol spectrometers. Since the days when electrical mobility techniques were used to study the properties of ionized gases, electrometers have been employed to detect and measure the concentrations of ions generated in the atmosphere and in the laboratory. In fact, early electric mobility instruments, such as the Whitby Aerosol Analyzer (WAA) and the Electric Aerosol Analyzer (EAA), used the Faraday cage of electrometers to measure the currents of charged particles downstream of classifiers.

The current measurements from each channel of the electrical mobility spectrometers are converted into the particle number concentration $N_{p,i}$ by the following relationship:

$$N_{p,i} = \frac{I_i}{g(n, d_p) \cdot \pi e \cdot Q_a} \quad 29$$

Here indicates the electrometer current on the spectrometer channel, $g(n, d_p)$ the probability of a particle whose diameter d_p carries n elementary charges, and Q_a the aerosol sample flow rate.

As shown in equation I.29, using electrometers to measure particle number concentrations has the disadvantage that the sensor response is weighted by the number of elementary charges carried by the particles. Indeed, a detailed model for predicting the distribution of charges on mono-dispersed particles is required for efficient conversion of current measurements into number concentrations. In addition, the sensitivity of the electrometer is very important, as it determines the concentration range the instrument can measure. In general, the electrometers used in aerosol instruments have a sensitivity of the order of a few femto amperes (fA), corresponding to monodisperse particle size concentrations of a few thousand particles cm^{-3} for the typical flow rates used by the instruments.

I.3 Conclusion

In this chapter, we have outlined general concepts regarding electrostatic precipitators, including their operating principles, the balance of forces acting on particles, charging mechanisms, particle movement, efficiency, and the various types of precipitators. The core principle of electrostatic precipitation involves charging particles by injecting electric charges into the air and then capturing them using electrostatic forces generated by an electric field in the inter-electrode space of the precipitator.

We have introduced a new technique for monitoring and controlling the flow of suspended particles in the filter. Additionally, a novel electrical collection system has been developed to measure the efficiency by assessing the electrical charge of the particles.

Industrial electrostatic precipitators typically operate using volume discharge at atmospheric pressure, with corona discharge being the most common due to its well-established

| General Information On Electrostatic Precipitators

advantages. However, citing some drawbacks of corona discharge, several researchers are exploring applications for dielectric barrier discharges.

CHAPTER II: The Methodological Choice

II.1 Introduction :

Electrostatic precipitation is a widely used process for removing solid (e.g. dust and ash) or liquid (e.g. oil mist) pollutants from gases released into the atmosphere [1,3]. Thanks to their low power consumption and high filtration efficiency (up to 99.9%), electrostatic precipitators are used in power stations and cement works, machine rooms in the wood and metalworking industries, office and residential buildings, hospitals, etc.... [4]. The development of ways of detecting aerosols and measuring the electrical charge of particles was mainly motivated by the need to find better ways of monitoring and controlling pollution [5,7].

This chapter is structured in two parts, with the aim of assessing filtration efficiency. The first part explores the use of the classical method, while the second part presents a new electrical aerosol capture system. This system detects particles suspended inside the capacitive electrostatic sensor (ECS) using a sensitive electrometer.

II.2 Experimental equipment and measurement methods

II.2.1 Electrostatic precipitator experimental set-up

The experimental set-up used for the study and electrical characterization of a filter is illustrated in figure II.1.

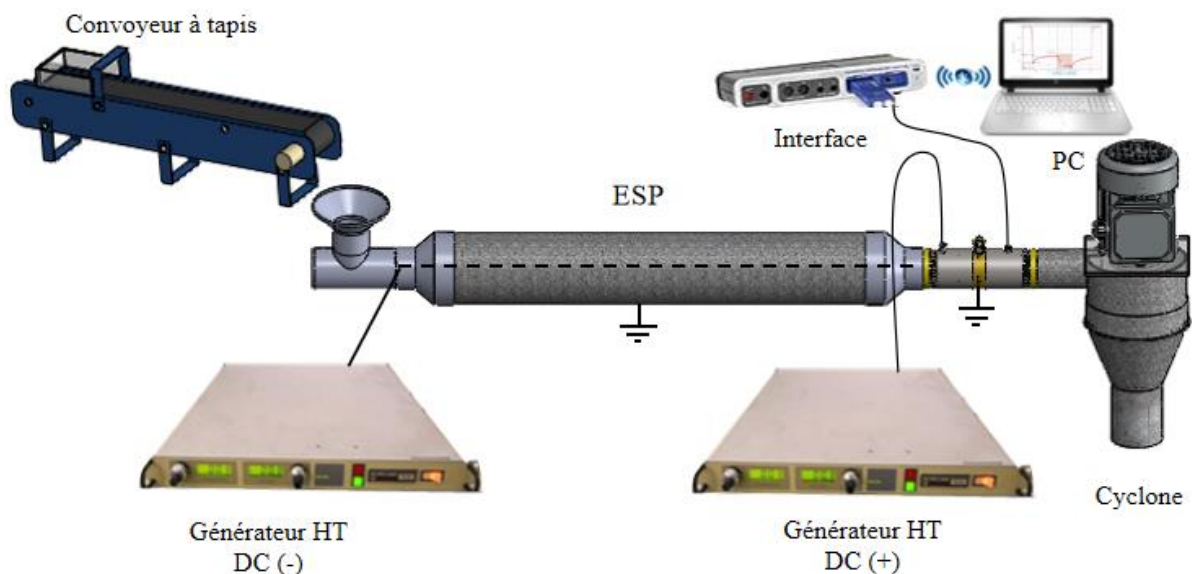


Figure II.1: General diagram of the experimental set-up

It comprises three distinct functional units:

- a. Powder inlet .
- b. Filtration device .
- c. Experimental equipment and instruments.

Each of these sections is described in detail below.

a) Description of the powder inlet section :

The ESP is supplied with powder by a conveyor belt, which introduces particles of silica fume with an average diameter of 63 μm , produced during the manufacture of silicon and ferrosilicon.

✓ Choice and characteristics of the powder used :

The choice of powder was not arbitrary: silica fume is extracted from the surface of the reduction furnace by main fans, and results from the condensation of SiO_2 gas, a reaction intermediate in the carboréduction process. It is then recovered and filtered through a bag filter and electrostatic precipitators, before being densified for easier handling.

The incorporation of silica fume into concretes leads to remarkable improvements in the rheological and mechanical characteristics of concretes. For fresh concretes, silica fume completes the granular spindle, eliminating any tendency to bleeding or segregation, while reducing the heat of hydration.

Particle size ranges from 40 to 63 μm (see Figure II.2).

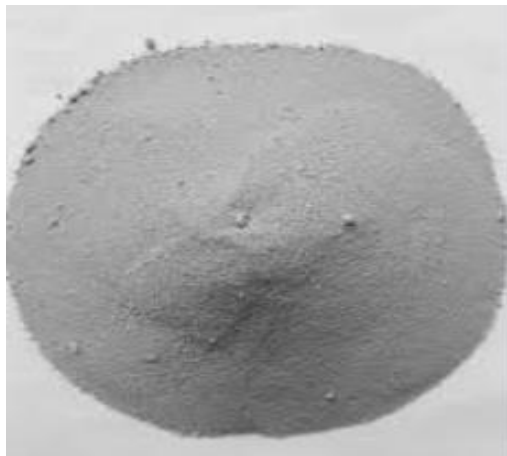


Figure II.2: Photograph of the silica fume microparticles used.

The flow velocity of the product inside the ESP is controlled by a cyclonic dust collector (maximum flow rate $Q_{\text{asp}} = 180 \text{ m}^3/\text{h}$) placed downstream of the filtration device, which also recovers the unfiltered powder. The filtration efficiency is estimated using the following classical equation :

$$n_1(\%) = \left[1 - \frac{m_s}{m_t} \right] \times 100$$

Where m_s and m_t are the unfiltered outgoing mass and the total introduced mass, respectively.

b) Filtration device :

The filtration device is a classic ESP "Fil-Cylindre" type in a horizontal position, comprising a grounded galvanized tube 700 mm long and 110 mm in diameter. The 0.25 mm diameter corona wire is connected to a high-voltage DC power supply from SPELLMAN, SL 300 series (± 40 kV; ± 7.5 mA), with an accuracy of 0.1 kV.

c) Experimental equipment and instruments..:

For this project, the group had access to a full range of laboratory equipment to carry out measurements and handle equipment under optimum safety conditions, ensuring the protection of group members and special apparatus. This equipment included generators (HV sources) and measuring instruments in perfect working order, enabling all experiments to be carried out without interruption or malfunction, and thus producing encouraging work with satisfactory results.

✓ **High Voltage Source**

This is a high-voltage DC generator from SPELLMAN, SL 300 series (± 40 kV; ± 7.5 mA), with an accuracy of 0.1 kV.



Figure II.3: Photograph of the high-voltage source

✓ **Electrometer :**

As shown in Figure II.1, the instrumentation section includes a sensitive PASCO-2132 electrometer (see Table II.1). This electrometer is connected on one side to a PASCO 550 universal interface, a multi-port USB data acquisition interface (see Figure II.4). This configuration enables PASCO Capstone software to be used to record and visualize data in real time on a microcomputer

Table II.1: Main characteristics of the load cell

Tension game	10 V with 500 μ V resolution
Load range	0.1 μ C with 5.0 pC resolution
Input capacity	0.01 μ F 5%
Input resistance	10^{12} ohms
Maximum input voltage	150 V DC, continuous
Input cable	shielded, 0.9m, alligator clip termination



Figure II.4: Photograph of P-2132 load cell and PASCO-550 interface

✓ **Thermal anemometer with propeller :**

Propeller anemometers are traditional wind measuring instruments widely used both indoors and outdoors. They are easy to use, enabling rapid measurement of wind or air speed. Many models also offer the option of measuring volumetric flow or temperature, facilitating data evaluation and comparison.



Figure II.5: Photograph of the thermal propeller anemometer - Precision propeller probe.

✓ **Precision thermo-hygrometer :**

This compact device measures relative humidity and temperature. Its sensor is wireless, enabling it to be moved from the unit using an intermediate connection cable. It enables remote monitoring of humidity and temperature.



Figure II.6: Photograph of the Testo precision thermo-hygrometer.

✓ **Electronic laboratory balance :**

The mass of the powder leaving or collected in the ESP of each experiment was measured to calculate the collection efficiency using an electronic balance with a resolution of 0.1g (Figure II.7).



Figure II.7: Photograph of the electronic laboratory balance.

✓ **Autotransformer :**

The use of the autotransformer (referenced as Figure II.8) allows us to regulate the speed of the cyclone by adjusting its supply voltage. The variation in flow velocity, noted "v", is obtained by modifying the supply voltage to the blower (V_{al}). The blower calibration process is carried out in the absence of discharge.



Figure II.8: Photograph of the auto-transformer.

✓ **Cyclone**

The cyclonic dust collector, located downstream of the filtration device, controls the flow speed of the unfiltered powder by means of a variable frequency drive.



Figure II.9: Photograph of the cyclone used.

II.2 New performance evaluation technique

In the industrial sector, electrostatic precipitators are often checked by opacimetric measurement. In a cement plant, for example, an opacimeter is placed at the gas outlet stack. A major problem with this measurement technique in mg/m^3 is the deposition of dust or ash, especially in the case of smoke, on the optical mechanism of the opacimeter, thus disrupting the measurement.

The aim is therefore to study the feasibility of a new efficiency evaluation system, which is in fact an electrostatic capacitive **ECS** sensor. The measurement is quantitatively accurate.

II.2.1 ECS electrostatic aerosol sensor

The **ECS** is a particle detection sensor located on the downstream side of the ESP; it consists of two parts. The first part is used to ionize particles by the corona effect, while the second, called the detection cell, relies on measuring the electrical charge of ionized particles.

II.2.2 Particle electrical charge measurement system

The charge measurement system includes our **ECS** capacitive electrostatic sensor, which is connected to a sensitive electrometer (Pasco-2121). This enables the evolution of electric charge to be visualized on a PC as a function of time, by measuring the electric charge during the flow of charged particles.

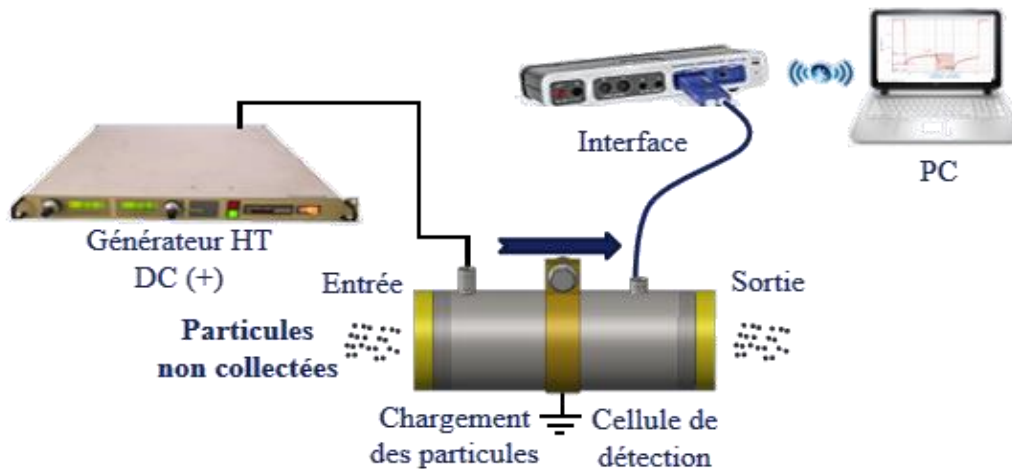


Figure II.10: Schematic diagram of the ECS capacitive electrostatic sensor

A) Particle feeder

The new particle detection system consists of two stages. In the first stage, a particle charger is used to electrically charge fine particles using a device based on the corona effect. This device comprises a needle-type active electrode, connected to a high-voltage power supply, and an internal grounded cylinder (40 mm in diameter). Positive corona discharges, generated in the vicinity of the active electrode, create a high ion space charge density between the needles and the inner cylinder. The ion stream then flows towards the ground electrode, making contact with the particles to be charged. Diffusion and field charging processes determine the final charge of the particles.

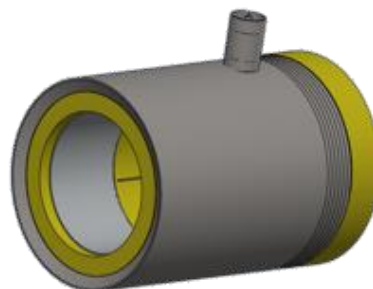


Figure II.11: Description of the corona charger.

B) Detection cell (electrical charge measurement)

In the second stage, the detection cell, which measures the electrical charge, receives the particles charged by the corona charger. The particles pass through two coaxial aluminum cylinders, separated by a 7 mm thick PTFE insulating tube. The outer cylinder, 100 mm long and 60 mm in diameter, is earthed, while the inner cylinder, 40 mm in diameter and containing the measuring point, is connected to a sensitive electrometer (Pasco). This electrometer is used to display on a PC the evolution of the electrical charge as a function of time.

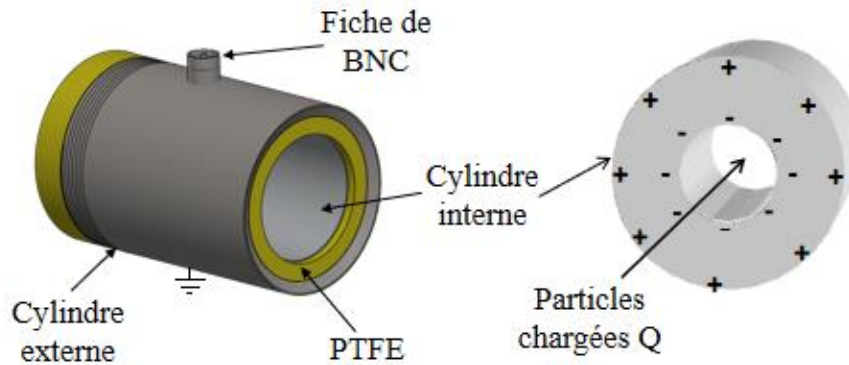


Figure II.12: Description of the detection cell

II.2.3 Load measurement method

The measurement technique used by our capacitive sensor is based on the measurement of the average total electric charge of the charged particles, given by the following relationship :

$$Q = C.V$$

The particles first pass through the particle charger. The charged particles flow through the detection cell, which measures the electrical charge by induction using a sensitive Pasco electrometer described above. The outer cylinder is grounded as a screen to prevent measurement of external charges, but also to reduce external electrical interference. A BNC plug is attached to the inner and outer cylinders, enabling the electrical load signal obtained via the Pasco Capstone to be displayed on a PC (Figure II.13).

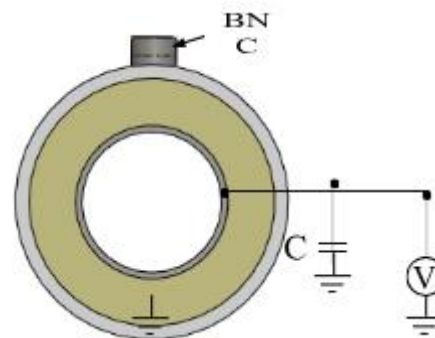


Figure II.13: Load measurement schematic diagram

II.2.4 Electrical charge measurement protocol

In order to experimentally test the reliability of our filter efficiency measurement technique, the same handling protocol was adopted for all tests (Figure II.14). The aim of these measurements is to determine the response of the ECS to particles leaving the ESP.

Before the silica fume particles are introduced, the corona charger is switched off for a period Δt_1 of 10 s. Immediately afterwards, the charger is switched on to monitor the evolution of the electrical charge by the detection cell over the same period Δt_1 . Immediately afterwards, the powder is injected for a time Δt_3 equal to 20 s (0.5g/s) and then stopped, with the charger source still energized. During this time, the detection cell (measuring the electrical charge) continuously records the variation in charge as a function of time for different situations.

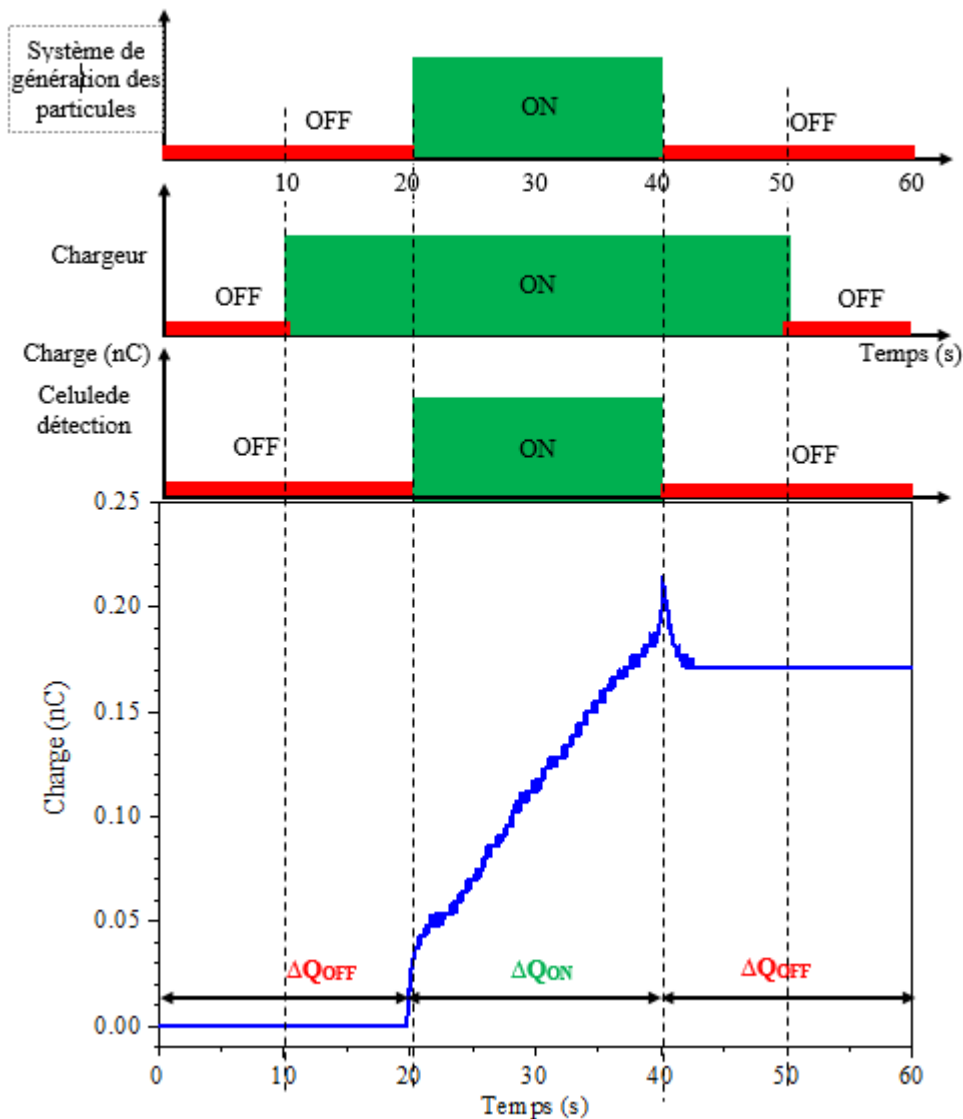


Figure II.14: Illustrative diagram of electrical charge measurement protocol

II.2.5 Experimental evaluation of electrostatic precipitator collection efficiency

The measurement protocol is valid for all experiments, and consists of plotting the variation in electrical charge as a function of time, for different levels of voltage applied to the ESP. The detection cell records the evolution of the charge as a function of time. A

typical diagram plotted by a sensitive PASCO electrometer connected to the PC is shown in figure II.15.

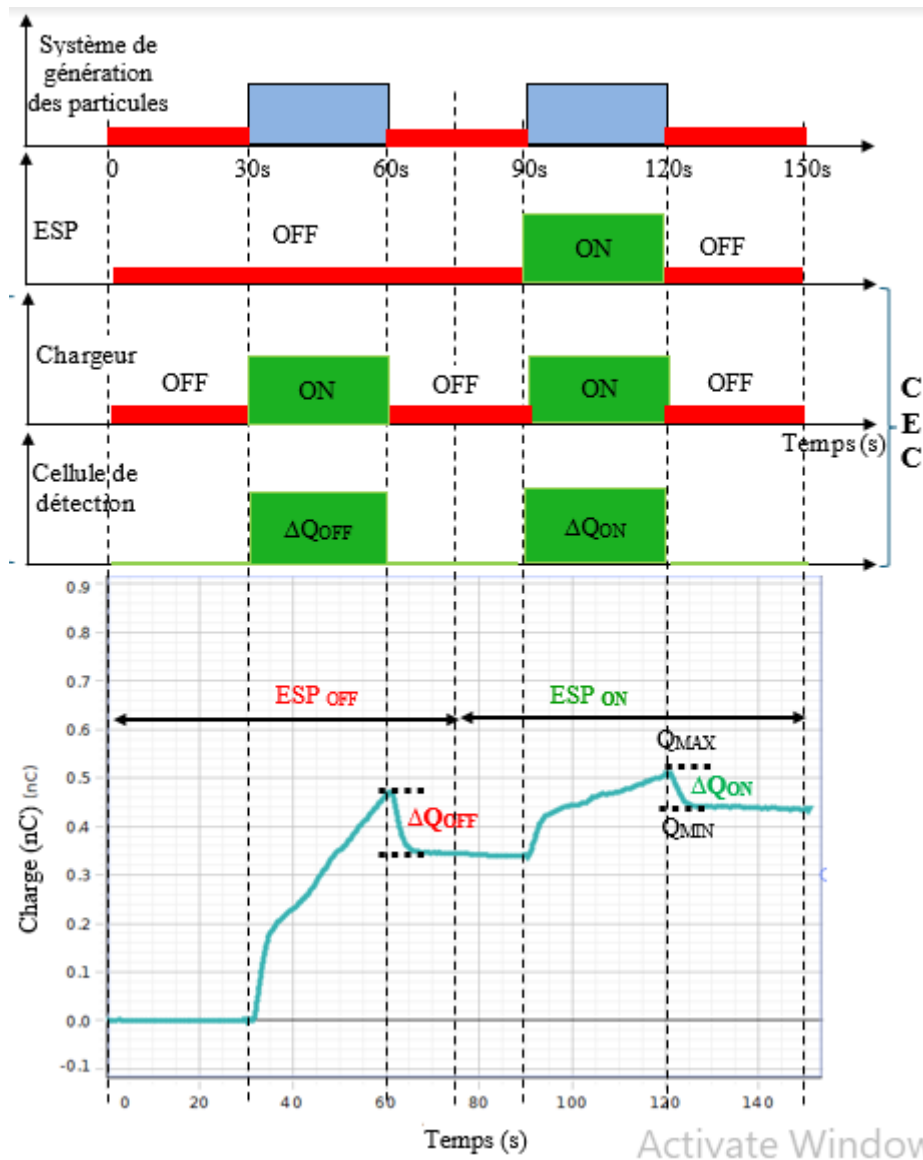


Figure II.15: Illustrative diagram of the protocol for evaluating the collection efficiency of an electrostatic precipitator.

The following relationship is proposed for evaluating filter efficiency and is given by by :

$$\eta_2(\%) = \left[1 - \frac{\Delta Q_{ON}}{\Delta Q_{OFF}} \right] \times 100$$

Where:

ΔQ_{OFF} : is the load difference recorded by the **ECS** when the ESP generator is OFF.

ΔQ_{ON} : is the charge difference recorded by the electrostatic sensor when the ESP generator is in the ON position.

The charge difference ΔQ at the electrostatic collector is given by the following equation :

$$\Delta Q \text{ (nC)} = Q_{\text{Max}} - Q_{\text{Min}}$$

II.3 Conclusion

In this chapter, we present a detailed description of the various experimental set-ups, including our sensor, as well as the performance evaluation technique based on electrical charge measurement.

Measurement protocols were adopted before and during our preliminary experiments in order to fine-tune our sensor, with the aim of obtaining the best possible sensitivity as the particle flow passes through the precipitators.

The next chapter will be devoted to analyzing and interpreting the results obtained in the laboratory, in order to assess the performance of our detection sensor.

CHAPTER III: Experimental Evaluation

III.1 Introduction

The submicrometric particles generated by industrial activities remain suspended in the air and have harmful effects on human health and the environment [14-16]. Consequently, the detection, sampling and counting of these particles using precise devices is of major importance in preserving air quality [6-7].

Instruments used for fine particle metrology measure concentration by number or mass per unit volume. They can detect a wide range of particle sizes, from a few nanometers to tens of micrometers, based on different physical principles; the most widely used are optical and electrical.

Using the electrical principle, measurement techniques are based on evaluation of the charge accumulated on particles, as with the Electric Low Pressure Impactor (ELPI) [13] or the Scanning Mobility Particle Sizer (SMPS) [9], among others. The optical principle is also used to detect aerosols larger than 0.18 μm in diameter in this field, as in the case of the CPC (Condensation Particle Counter) or the Aerosol Spectrometer [10-11].

However, the major problem with these devices is their mode of operation, i.e. they cannot be placed continuously in filtration systems, due to saturation and the risk of damage to their optical components.

In this chapter, we will test our ECS capacitive electrostatic sensor to evaluate the capture efficiency of submicrometer particles.

III.2 Assessment of collection efficiency by the classical method

The measurement protocol is valid for all experiments. It consists of plotting the variation in efficiency as a function of high voltage, for different study parameters, i.e. the high voltage applied, and the mass flow rate of the pollutant.

When a voltage exceeds a certain threshold (discharge ignition voltage), a corona discharge forms around the wire. The ions generated by this discharge pass through the inter-electrode gap under the effect of a DC electric field, in the direction of the collecting electrode. When silica fume particles are introduced into the electrofilter at a velocity of 0.5 g/s, they pass through the inter-electrode gap. Along the way, these particles capture

Experimental Evaluation

ions and become strongly charged, subjecting them to the Coulomb force, attracting them to the ground electrode. The collected dust is then recovered by a mechanical process that consists of striking the wall of the electrofilter with a hammer. Filtration efficiency is estimated using the classical equation :

$$\eta_1(\%) = \left[1 - \frac{m_s}{m_t} \right] \times 100$$

Where m_s et m_t are the unfiltered outgoing mass and the total introduced mass, respectively.

As we used a specific quantity of particles ($m=10$ g), the tests were carried out under the following conditions: temperature 25.5°C and humidity 52%.

Table III.1: Efficiency as a function of tension for ESP

Voltage (kV)	Collection weight (g)	Outgoing mass (g)	Yield (%)
12	4.10	5.74	41
14	5.80	4.10	58
16	7.40	2.45	74
18	8.70	1.19	87
20	9.6	0.2	96

Figure III.1 shows the simultaneous variation in filter efficiency η as a function of voltage V_{ESP} for a suction flow rate $Q_{ASP} = 2.1$ m/s.

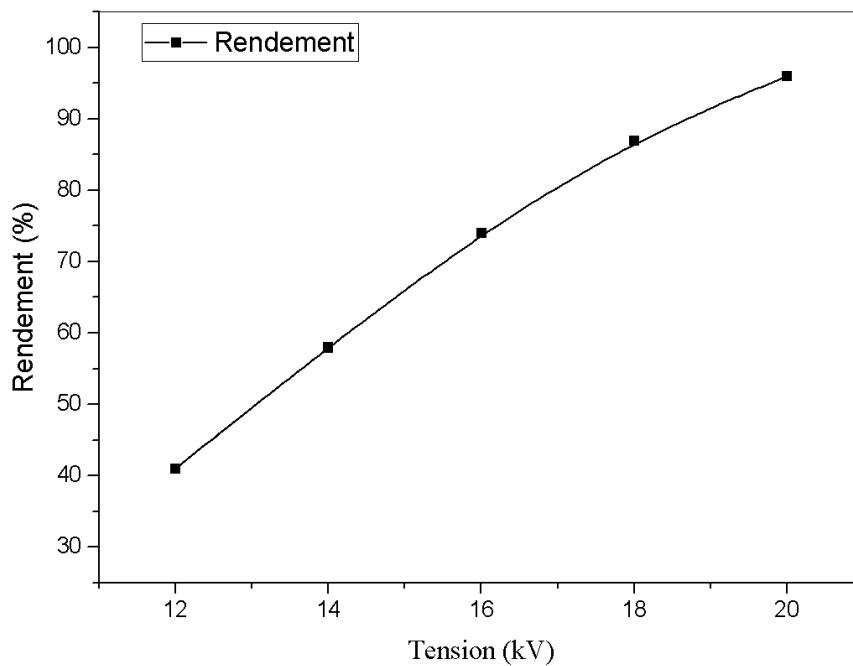


Figure III.1: Simultaneous variation of efficiency as a function of voltage ($Q_{ASP} = 2.1m/s$)

The results shown in Figure III.1 indicate that the increase in efficiency is indeed obtained by increasing the applied voltage. On the other hand, the outgoing mass is inversely proportional to the voltage.

III.2 Assessing collection efficiency by measuring electrical charge

III.2.1 ECS particle detection technique

The ECS determines the polarity of the total electrical charge Q and detects the presence of aerosol at the electrostatic filter outlet.

Figure III.2 illustrates typical examples of the evolution of electrical charge Q as a function of time for voltage $V_{CH} = 14$ kV applied at the particle charger level (1^{ier} ECS stage) was chosen after a series of preliminary experiments (figure III.3). The charge difference ΔQ represents the total electrical charge of the particles as they leave the ECS. It is evaluated by the following relationship:

$$\Delta Q = Q_{MAX} - Q_{MIN}$$

Where Q_{MAX} and Q_{MIN} are the electrical charges of the particles.

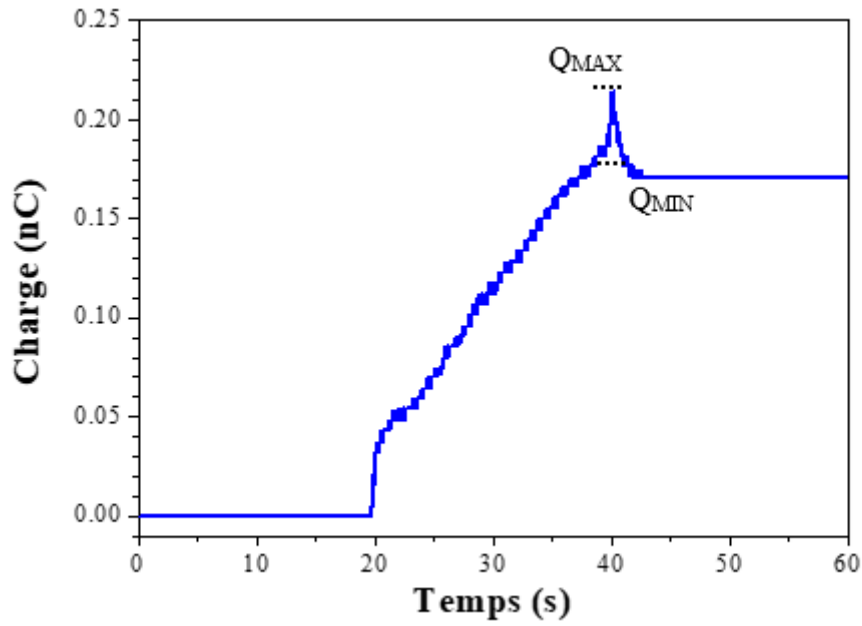


Figure III.2: Typical diagram showing the evolution of electrical charge as a function of time for a voltage of 14 kV

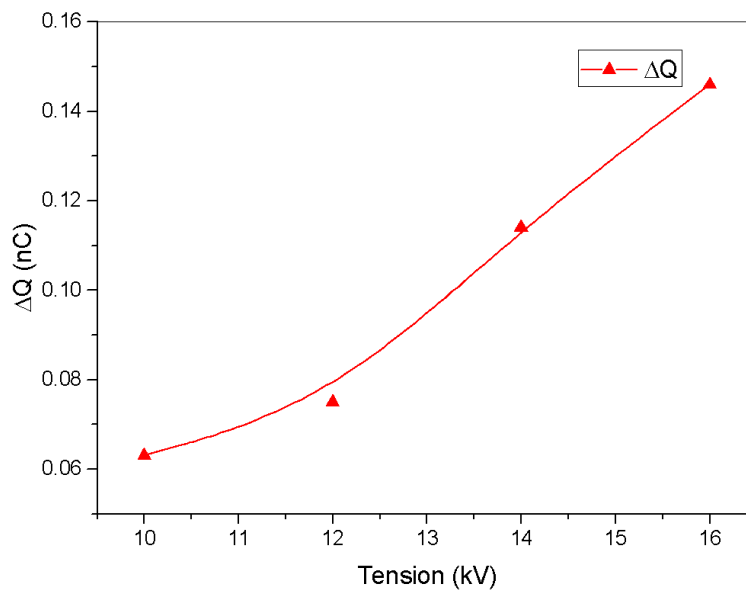


Figure III.3: Typical diagram showing the evolution of electric charge as a function of voltage V_{CH} for a mass of 0.5 g.

III.2.2 Evaluation of collection efficiency using the charge difference technique ΔQ

In order to confirm the results of the electrical load measurement with the capacitive sensor, the collection efficiency of the ESP, composed of a crown discharge ESP in DC voltage, was estimated.

Figure III.4 shows the variation curve of the electrical load as a function of time for a voltage $V_{ESP} = 12$ kV and a fixed voltage $V_{CH} = 14$ kV . Different values of DC voltage at the ESP have been applied ($V_{ESP} = 12$ kV, 14 kV, 16 kV, 18 kV and 20 kV). This is done to create an electric field in the inter-electrode space to trap charged particles for good ESP monitoring. The **ECS** downstream of the ESP is used to monitor and estimate the collection efficiency using the following relationship:

$$\eta_2 (\%) = [1 - \frac{\Delta Q_{ON}}{\Delta Q_{OFF}}] \times 100$$

Where:

ΔQ_{OFF} : is the difference in electrical charge of the particles when the ESP generator is in the OFF position.

ΔQ_{ON} : is the difference in electrical charge of the particles when the ESP generator is in the ON position.

The charge difference at the **ECS** $\Delta Q_{ON} = 0.072$ nC for a voltage $V_{ESP} = 12$ kV (Figure III.4), becomes $\Delta Q_{ON} = 0.032$ nC for $V_{ESP} = 16$ kV (Figure III.5) and $\Delta Q_{ON} = 0.011$ nC for $V_{ESP} = 20$ kV (Figure III.6).

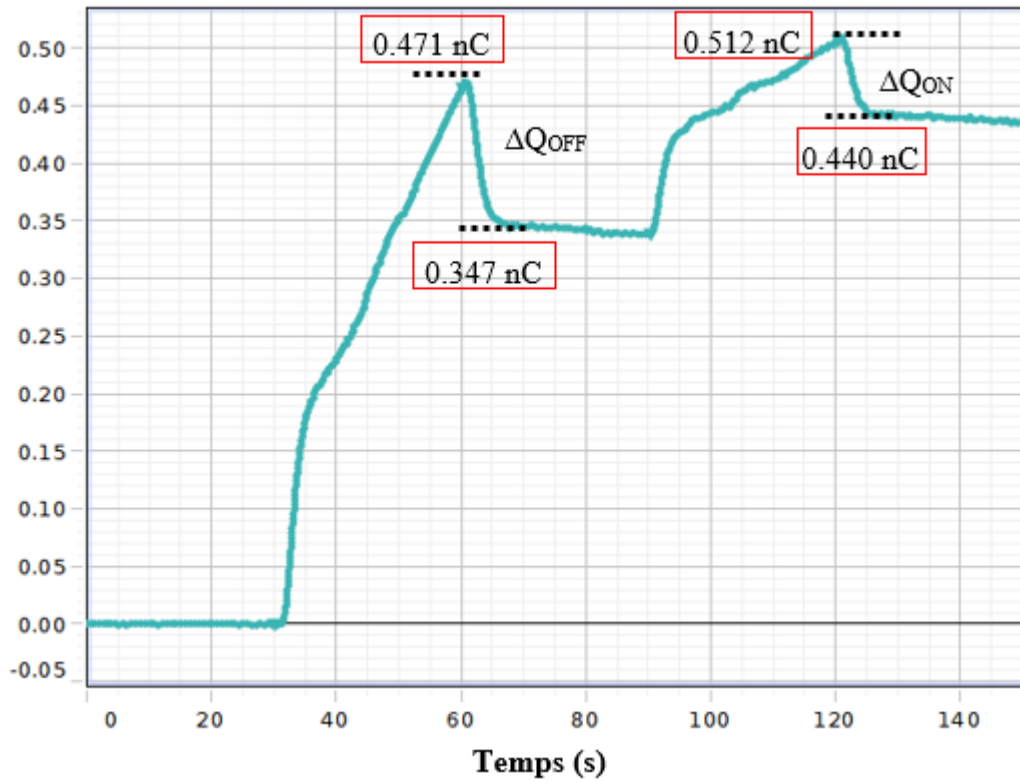


Figure III.4: Load vs. time variation for ($V_{CH} = 14$ kV, $V_{ESP} = 12$ kV)

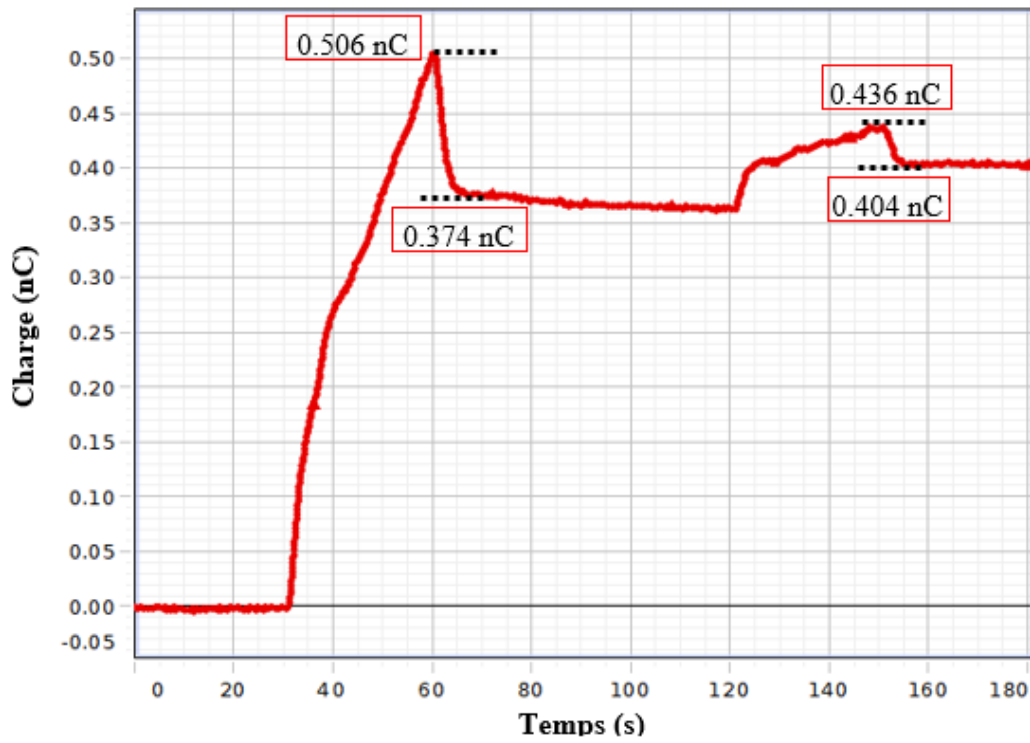


Figure III.5: Load vs. time variation for ($V_{CH} = 14$ kV, $V_{ESP} = 16$ kV)

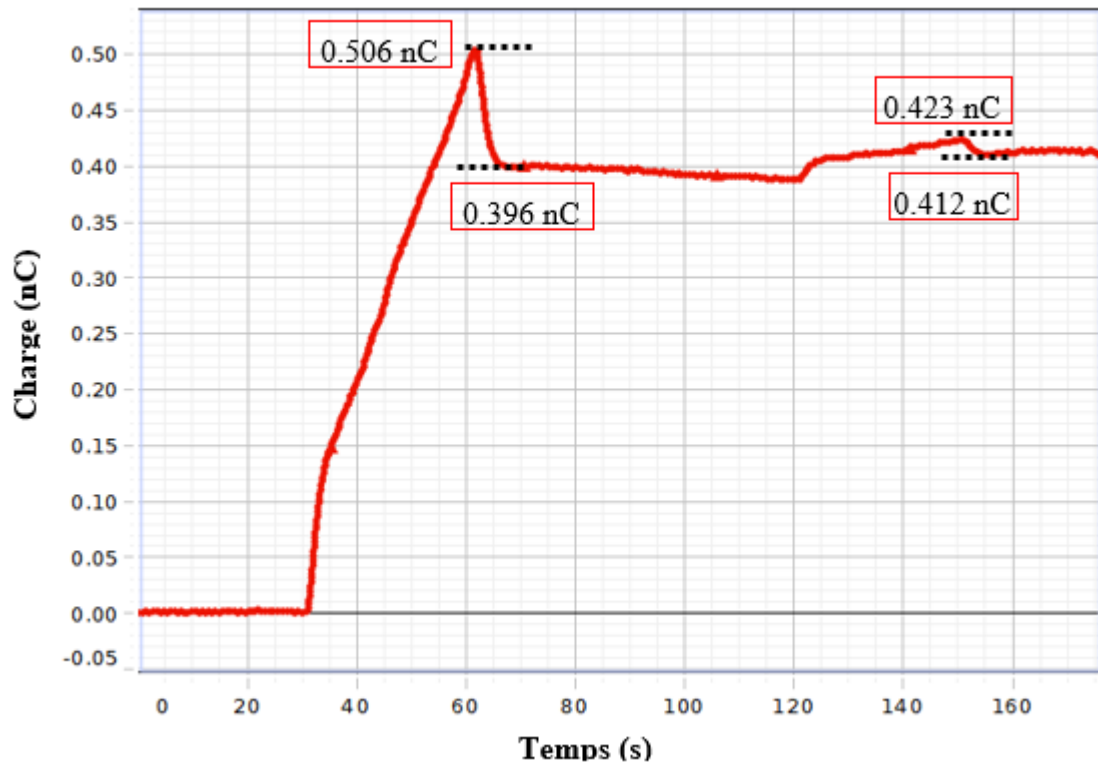


Figure III.6: Load vs. time variation for ($V_{CH} = 14 \text{ kV}$, $V_{ESP} = 20 \text{ kV}$)

The collection efficiency of our filter was compared with that obtained using the classical relationship. Figure III.7 clearly shows the variation in collection efficiency as a function of V_{ESP} by the two calculation methods used. The results obtained show almost perfect agreement between efficiency measured electrically using the capacitive sensor connected to a sensitive electrometer and by classical measurement. An analogy between the two curves makes it possible to identify the value of the constant k that exists between the two measurement techniques. We can therefore establish a relationship between the two efficiency formulas, given by :

$$\eta(\%) = \eta_1(\%) = k \times \eta_2(\%)$$

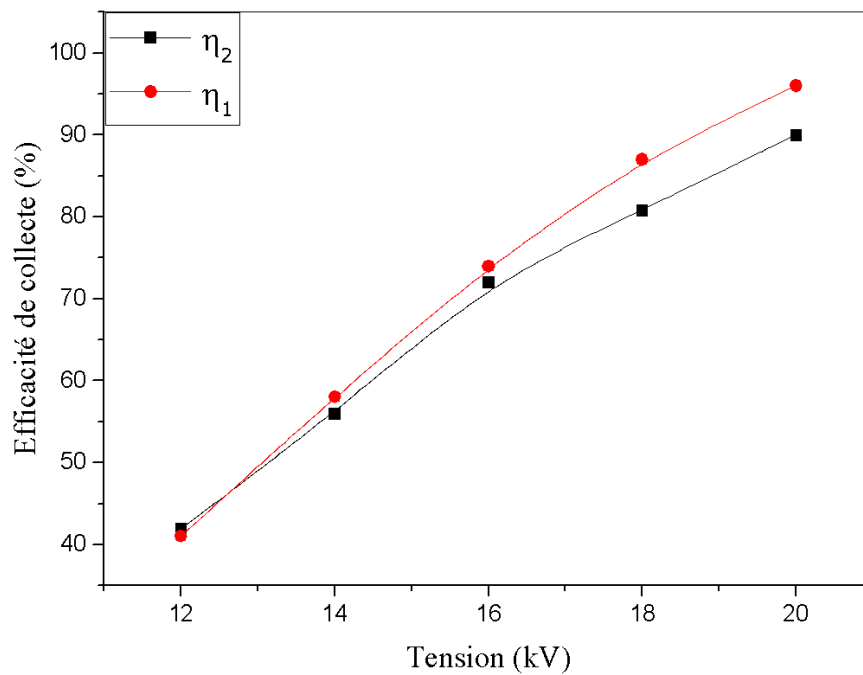


Figure III.7: Comparative curves for calculating collection efficiency as a function of $V_{.ESP}$

III.3 Conclusion

An experimental analysis has been carried out in this chapter to validate a new technique for particle detection and operational control of an electrostatic filter. This method is based on measuring the electrical charge of particles ionized by the corona charger using a sensitive electrometer.

The results obtained showed that this new method gives precise measurement values and enables good monitoring of an electrostatic process such as dust or fume filtration.

General Conclusion

IV.1 General Conclusion

Electrostatic precipitation has proved to be the most effective particle collection technique among existing aerosol treatment processes. Generally speaking, industrial electrostatic precipitators use a volume discharge at atmospheric pressure. The most widespread is the negative polarity corona discharge, whose advantages are well established. These clean techniques are subject to numerous constraints (economic, technical and legal), which must be respected in order to protect our environment from pollution.

Nevertheless, the operation of these filters is not always stable, and fluctuations in filtration efficiency frequently occur, requiring the installation of a reliable monitoring and measurement system in continuous operation downstream of the ESP. Consequently, the detection, sampling and counting of these particles using precise instruments is of paramount importance in preserving air quality.

To this end, an electrostatic particle detector (EPD) located downstream of the electrostatic precipitator has been developed to monitor particles leaving the ESP. In addition, this new detection system makes it possible to measure efficiency accurately and without intermittence. This technique is based on measuring the electrical charge caused by particles suspended in the detection cell without being collected, which keeps the sensor clean at all times and therefore reduces cleaning frequency.

The particle detection system we have proposed, consisting of a capacitive electrostatic ECS sensor and a sensitive electrometer, is based on the measurement of the electrical charge of particles, charged by the corona effect.

IV.2 Perspectives

- At the end of this study, we can conclude that the instruments and measurement techniques we have proposed and successfully tested can find a place among the existing instruments on the market.
- Calibration and comparison of capacitive sensors with other particle measurement devices such as SMPS, CPC, PPS....
- In order to better monitor the transient behavior of airborne particles, we need to further improve the use of prototypes, particularly for fine particles.

Bibliographical References

Bibliographical references

- [1] S.A. Hoenig, “New application of electrostatic technology to control of dust, fumes, smokes and aerosols”, *IEEE Trans. Ind. Appl.*, 17, pp. 386–391, 1981.
- [2] J.B. Gajewski, “Monitoring of electrostatic fire and explosion hazards at the inlet to electrostatic precipitators”, *Journal of Electrostatics* Vol. 72: 192-197, 2014.
- [3] J. H. Vincent, “Aerosol Sampling: science, standards, instrumentation and application”, (Chichester: John Wiley & Sons edition), 2007.
- [4] W. C. Hinds, “Aerosol Technology: Properties, Behavior and Measurement of Airborne Particles”, New York: 2nd Edition, Wiley - Interscience, 1999.
- [5] P. Intra and N. Tippayawong, “Particle Size Analyzers”. *Journal of the Scientific & Technological Research Equipment Centre*, Vol. 11, pp. 156-170, (in Thai), 2003.
- [6] P. Intra and N. Tippayawong, “An Overview of Aerosol Particle Sensors for Size Distribution Measurement”, *Maejo International Journal of Science and Technology*, Vol. 1, No. 2, pp. 120 – 136, 2007.
- [7] B. Dramane, “Précipitation électrostatique de particules submicronique par décharge à barrière diélectrique – étude électrique, granulométrique et aérodynamique”, Thèse de Doctorat, Université de Poitiers, 2009.
- [8] TSI Incorporated. Operation and Service Manual, Revision L, for Scanning Electrical Mobility Sizer™ (SMPS™) Spectrometer, Model 3936, Minnesota, 2006.
- [9] J. K. Agrawal and G. J. Sem. Continuous Flow, “Single-particle-counting Condensation Nucleus Counter”. *Journal of Aerosol Science*, Vol. 11, pp. 343 – 357, 1980.
- [10] TSI Incorporated. Instruction Manual, Revision F, for “Condensation Particle Counter”, Model 3010, Minnesota, 2002.
- [11] T. Johnson, S. Kaufman and A. Medved, “Response of an Electrical Aerosol Detector based on a Corona Jet Charger”, 6th International. ETH Conference Nanoparticle Measurement, 19 – 21 August, Zurich, Switzerland, 2002.
- [12] J. Keskinen, K. Pietarinen and M. Lehtimäki, “Electrical Low Pressure Impactor”, *Journal of Aerosol Science*, Vol. 23, pp. 353-360, 1992.
- [13] COMMISSION DE LA PRODUCTION ET DES ÉCHANGES, “La pollution de l’air”, Technical report, Rapport d’Information N°3088 de l’Assemblée Nationale, 23 Mai 2001, <http://www.assemblee-nationale.fr/rap-info/i3088.asp>, 2001
- [14] A. D. Kappos et al., “Health effects of particles in ambient air”, *International Journal of Hygiene and Environmental Health*, vol. 207, pp. 399-407, 2004.
- [15] I. M. Kennedy, “The health effects of combustion-generated aerosols”, *Proceedings of the Combustion Institute*, Vol. 31, pp. 2757-2770, 2007.
- [16] C. S. Tang, L. T. Chang, L. C. Lee, and C. C. Chan, “Effects of personal particulate matter on peak expiratory flow rate of asthmatic children”, *Science of the Total Environment*, vol. 382, pp. 43-51, 2007.
- [17] R. Gouri, “Optimisation électrique et géométrique d'un électrofiltre à barrière

- diélectrique en configuration fil-tube carré application aux particules submicroniques”, Poitiers, France: Thèse de Doctorat, Université de Poitiers, 2012
- [18] H. J. White, “Industrial Electrostatic Precipitation”, Wesley Publishing Company, Inc, 1963.
- [19] A. Mizuno, “Electrostatic precipitation”, IEEE Transactions on Dielectrics and Electrical Insulation, Vol. 7, No. 5, pp. 615–624, 2000.
- [20] K. R. Parker, “Electrostatic precipitation”, Chapman & Hall, 1997.
- [21] J.S. Chang, A.J. Kelly, J.M. Crowley, “Handbook of Electrostatic Processes” Marcel Dekker, New York, 1995.
- [22] T. J. Krinke, K. Deppert, M. H. Magnusson, F. Schmidt, H. Fissan, “Microscopic aspects of the deposition of nanoparticles from the gas phase”, Journal of Aerosol Science, Vol. 33, No. 10, pp. 1341–1359, 2002.
- [23] C. U. Böttner, “The role of the space charge density in particulate processes in the example of the electrostatic precipitator”, Powder Technology, Vol. 135–136, pp. 285–294, 2003.
- [24] R. Boichot, “Filtration des particules issues des moteurs diesel par matrices fibreuses plongées dans un champ électrique”, Thèse de Doctorat de l’Université de Savoie, 2005.
- [25] C. Riehle, Basic and theoretical operation of ESPs. London: Electrostatic precipitation. Chapman & Hall, 1997.
- [26] G. Artana, G. Touchard, M.F. Morin, “Contribution to the analysis of the flow electrification process of powders in pneumatic conveyers”, Journal of Electrostatics, Vol. 40–41, pp. 277–282, 1997.
- [27] G.0 Touchard, S. Sammartino, G. Artana, F. Putier, S. Watanabe, “Technologie des pulvérulents dans les IAA - Chapitre 5 : Caractérisation électrique des milieux granulaires”, Editions Tec & Doc, Paris, pp. 119-153, 2003.
- [28] Z. Sternovsky, A. Sickafoose, J. Colwell, S. Robertson, M. Horányi, “Contact charging of Lunar and Martian dust simulants”, Journal of Geophysical Research, Vol. 72, No. 11, pp. 5105, 2002.
- [29] H. Pang, “Dépoussiérage électrostatique pour les particules submicroniques en atmosphère usuelle (terre) et rarifiée (planète Mars)”. Grenoble, France: Thèse de Doctorat, Université Joseph FOURIER-Grenoble 1, 2006.
- [30] A. Bouarouri, “Développement d’un chargeur à décharge couronne pour la mesure à 10 Hz de la concentration d’aérosol atmosphérique”, Paris, France: Thèse de Doctorat, Université PARIS-SUD, 2014.
- [31] P. Tochon, “Étude numérique et expérimentale d’électrofiltres industriels”, Thèse de doctorat de l’Université Joseph Fourier, 1997.
- [32] J. A. Cross, “Electrostatics, principles, problems and applications”, Edition Adam Hilger, Bristol, 1987.

Bibliographical references

- [33] H. Rohmann, "Methode zur messung der grÖÙe von schwebeteilchen", *Zeitung der Physik*, vol. 17, pp. 253-265, 1923.
- [34] M. Pauthenier and R. Guillien, "Etude électromécanique de la charge limite d'une sphère conductrice dans un champ électrique ionisé", *C.R.A.S. Paris*, vol. 195, 1932.
- [35] M. Pauthenier and M. Moreau-Hanot, "La charge des particules sphériques dans un champ ionisé", *Journal de Physique et le Radium*, vol. 3, pp. 590-613, 1932.
- [36] J. R. Brock, "Non continuum unipolar charging of aerosol: the role of external electric field", *Journal of Applied Physics*, vol. 41, pp. 1940-1944, 1970.
- [37] J. R. Brock and M. Wu, "Field charging of aerosol particles", *Journal of Colloid and Interface Science*, vol. 45, pp. 106-114, 1973.
- [38] B. H. Y. Liu and D. H. Y. Pui, "On polar diffusion charging of aerosol in the continuum regime", *Journal of Colloid and Interface Science*, vol. 58, No. 1, pp. 142-149, 1977.
- [39] A. Mizuno, "Contact-type electric curtain for electrodynamic control of charged dust particles", in *Proc. 1st International Conference on Electrostatic Precipitation*, 1981.
- [40] J. R. MacDonald, "A mathematical model for calculating electric conditions in wireduct electrostatic precipitation", *Journal of Applied Physics*, vol. 48, No. 6, pp. 2231-2243, 1978.
- [41] J. P. Borra, "Nucleation and aerosol processing in atmospheric pressure electrical discharges: powders production, coatings and filtration", *Journal of Physics D: Applied Physics*, vol. 39, pp. R19-R54, 2006.
- [42] N. A. Fuchs, "The charges on the particles of aerocolloids", *Izvestiya Akademii Nauk SSSR Seriya Geograficheskaya*, vol. 11, p. 341, 1947.
- [43] N. A. Fuchs, "On the stationary charge distribution on aerosol particles in a bipolar ionic atmosphere", *Geofisica Pura e Applicata*, vol. 56, p. 185, 1963.
- [44] H. J. White, "Particle charging in electrostatic precipitation", *AIEE Transactions*, vol. 70, pp. 1186-1191, 1951.
- [45] P. A. Lawless and E. J. Shaughnessy, "Laser doppler anemometer measurements of particle velocity in a laboratory precipitator", in *IEEE Industry Applications (IAS) Annual Meeting*, p. 1124, 1981.
- [46] P. A. Lawless, "Particles charging bounds, symmetry relations and analytic charging rate model for continuum regime", *Journal of Aerosol Science*, vol. 27, pp. 191-215, 1996.
- [47] P. A. Lawless and R. F. Altman, "Espm: an advanced electrostatic precipitator model", in *29th IEEE Industry Applications (IAS) Annual Meeting*, Denver, 1994.
- [48] W. B. Smith and J. R. McDonald, "Development of a theory for the charging of particles by unipolar ions", *Journal of Aerosol Science*, vol. 7, pp. 151-166, 1976.
- [49] R. Cochet, "Loi de charge des fines particules (submicroniques)", in *Colloque International N°102 : La physique des forces électrostatiques et leurs applications*, C.N.R.S., Paris, Paris, pp. 331-338, 1961.

Bibliographical references

- [50] D. Brocilo, J. S. Chang, and R. D. Findlay, "Modeling of electrode geometry effects on dust collection of wire-plate electrostatic precipitators", in 8th International Conference on Electrostatic Precipitation ICESP, Birmingham, Alabama, USA, 2001.
- [51] B. J. Yoon, "Continuum theory for ionic field charging of spheroidal aerosols in nonuniform electric field", *Chemical Engineering Science*, vol. 55, pp. 5485-5495, 2000.
- S. Oglesby and G.B. Nichols, *Electrostatic Precipitation*. New York: Marcel Dekker, Inc., 1978.



الجمهورية الجزائرية الديمقراطية الشعبية

وزارة التعليم العالي والبحث العلمي

جامعة عين تموشنت بلحاج بوشعيب

حاضنة الأعمال عين تموشنت



ملحق نموذج العمل التجاري

BOUSSAID Issam Mohamed Ali بوسعيد عصام محمد علي	الاسم و اللقب Your first and last Name
ECS (electrostatic capacitive sensor)	الاسم التجاري للمشروع Title of your Project
0540075715	رقم الهاتف Your phone number
boussaid.issam01@gmail.com	البريد الالكتروني Your email address
Ain Temouchent عين تموشنت	(مقر مزاولة النشاط) الولاية- البلدية Your city or municipality of activity

Project technical document

Nature of the project :

The Product Has a Productive and a Serviceable Nature

1-The Problem to be Solved Supported by Data

Air pollution is a growing concern due to its detrimental impact on human health and the environment. Aerosol particles, which include dust, pollen, soot, smoke, and liquid droplets, play a significant role in air quality. Monitoring the concentration and size distribution of these particles is critical for developing strategies to reduce exposure to harmful pollutants.

Traditional methods for aerosol detection often rely on optical and gravimetric techniques, which, while effective, can be expensive, require frequent maintenance, and may not provide real-time data. Therefore, there is a growing interest in developing more efficient, cost-effective, and portable methods for monitoring aerosol particles in real time. Electrostatic and capacitive sensing technologies offer promising alternatives due to their ability to detect changes in particle concentration through electrical properties, potentially leading to more accessible pollution monitoring systems.

Here are some key statistics related to air pollution and its global impact:

1. **Global Deaths:** Air pollution is responsible for approximately 7 to 8.1 million premature deaths annually, making it the second leading risk factor for death globally. It primarily contributes to diseases such as ischemic heart disease, stroke, chronic obstructive pulmonary disease (COPD), lung cancer, and acute respiratory infections like pneumonia
2. **Impact on Children:** In 2021, over 700,000 deaths in children under the age of five were linked to air pollution, representing about 15% of global child mortality for that age group
Economic Costs: Air pollution imposes significant economic burdens, accounting for 6.1% of the global GDP, or over \$8 trillion in 2019, due to healthcare costs and productivity losses.
3. **Exposure Levels:** Around 99% of the global population is exposed to air pollution levels exceeding the World Health Organization's (WHO) recommended guidelines

These statistics underline the importance of developing accessible and cost-effective technologies, like the electrostatic and capacitive sensors described in your project, to monitor and combat the effects of air pollution in real time.

2-Our Offer

We provide a comprehensive solution for detecting and monitoring aerosol particle density using advanced electrostatic and capacitive sensor technology. Our offer includes:

1. **State-of-the-Art Sensor Technology**

We supply high-precision sensors capable of detecting aerosol particles in real time. These sensors are designed for a wide range of environments, from industrial settings to urban air monitoring, ensuring accurate and reliable data collection.

2. **Turnkey Monitoring System**

Our offer includes a fully integrated system that combines hardware and software for seamless operation. Clients receive a complete solution for air quality monitoring, including data analysis tools that provide actionable insights.

3. **Installation and Setup**

We handle the installation and initial setup of the sensors, ensuring that the system is correctly calibrated and operational from day one. Our technical team ensures the system integrates smoothly with existing infrastructure.

4. **Maintenance and Support**

Our offer includes ongoing **maintenance** services to ensure the long-term functionality and accuracy of the monitoring system. With low-maintenance sensors, clients benefit from minimal disruptions, and our support team is available to assist with any technical issues or updates.

5. **Real-Time Data and Analytics**

The system will offers real-time data access via a user-friendly interface, allowing clients to monitor air quality in real time and receive alerts for any critical changes. The integrated analytics platform provides detailed reports and trends to support decision-making.

3-The Value We Bring to the Client

1. **Technical Expertise**

Leveraging our in-depth expertise in aerosol particle detection and measurement, we provide the client with state-of-the-art air quality monitoring solutions. Our electrostatic and capacitive sensors offer precise particle detection, ensuring real-time monitoring and reliable data.

2. **Innovation and Reliability**

By using innovative and proven technologies, we offer an alternative to traditional methods that are often expensive and complex. Our sensors are designed to be efficient and energy-saving, providing continuous monitoring that

can be adapted to various environments while minimizing maintenance and calibration requirements.

3. **Cost-Effectiveness and Accessibility**

Our goal is to deliver affordable, scalable solutions that make air quality monitoring accessible to a broader range of industries and applications. This cost-effective approach ensures that clients can deploy these systems widely without compromising on performance or accuracy.

4. **Low Maintenance and Longevity**

One of the key advantages of our sensors is their **low maintenance** needs. The robust design and durable materials used ensure that the system operates effectively for extended periods with minimal intervention. This reduces downtime and lowers long-term operational costs for the client. The system also features self-diagnostics and requires infrequent calibration, making it easy to maintain in any setting.

5. **Real-Time Data for Informed Decision-Making**

Our sensors deliver real-time data, enabling clients to make informed, timely decisions regarding air quality management. Whether for industrial, environmental, or public health applications, this real-time insight helps clients take proactive measures to mitigate pollution and improve air quality.

4-Our Clients

We cater to a diverse range of clients who require reliable and efficient air quality monitoring solutions. Our clients include:

1. **Environmental Agencies**

Government agencies and environmental organizations tasked with monitoring air quality on a regional or national scale use our solutions to gather accurate data on aerosol particles and pollution. Our system helps them track pollution trends, comply with environmental regulations, and enforce air quality standards.

2. **Industrial Companies**

Industries such as manufacturing, mining, and energy production rely on our sensors to monitor emissions and ensure compliance with environmental regulations. By using our system, they can detect harmful aerosol particles and reduce their environmental footprint while protecting workers' health.

3. **Research Institutions**

Universities and research centers conducting studies on air pollution, climate change, or health impacts of aerosols benefit from our high-precision monitoring

systems. Our technology provides them with reliable, real-time data to support their research and contribute to scientific advancements.

4. **Public Health Organizations**

Health organizations concerned with air pollution's impact on public health use our monitoring solutions to assess pollution levels and correlate data with respiratory illnesses and other health conditions. This helps them inform policy decisions and public health interventions.

5. **Construction and Demolition Companies**

Companies in the construction and demolition industries utilize our air quality monitoring solutions to measure dust and particulate matter during operations, ensuring they stay within legal limits and avoid negative environmental impact. This also helps them reduce health risks to workers and neighboring communities.

6. **Energy and Utilities Sector**

Companies in energy production (e.g., power plants, refineries) often emit particles as byproducts. Our solutions allow them to monitor and control these emissions to meet regulatory standards and improve sustainability efforts.

5-Client Relationship Management

Our approach to client relationships is centered on building trust, delivering value, and ensuring long-term satisfaction. We prioritize the following elements:

1. **Personalized Support**

We believe in tailoring our interactions to each client's specific needs. From the initial consultation to the final deployment, our team works closely with clients to understand their challenges and provide solutions that best fit their requirements. This personalized approach ensures that clients receive exactly what they need for optimal results.

2. **Proactive Communication**

We maintain regular, open lines of communication with our clients. This means not only responding to their requests and concerns in a timely manner, but also proactively updating them on new features, system enhancements, and industry developments. Regular check-ins help us stay aligned with our clients' evolving needs.

3. **Dedicated Account Management**

Each client is assigned a dedicated account manager, who acts as their primary point of contact. This ensures that clients always have a direct line to someone who understands their business and can address their needs quickly and

effectively. The account manager is responsible for overseeing the entire relationship, from onboarding to long-term support.

4. **Continuous Support and Maintenance**

Our commitment to the client extends beyond the initial installation. We offer continuous support through maintenance packages, system health checks, and technical assistance. Should any issues arise, our support team is available to troubleshoot, ensuring minimal disruption to operations. Regular system updates also ensure that clients always have access to the latest technology.

5. **Feedback and Improvement**

We value client feedback as it helps us improve our products and services. Through surveys, feedback sessions, and post-project reviews, we actively seek client input on their experience. This allows us to adapt and enhance our offerings to better serve future client needs.

6. **Long-Term Partnership**

Our goal is to establish long-term partnerships with our clients, providing not only immediate solutions but also planning for future needs. By offering scalable systems and flexible solutions, we ensure that as the client's business grows or their needs evolve, our technology can adapt alongside them.

7. **Client Success Program**

We implement a client success program that tracks and measures the success of the solutions deployed. Our team regularly checks in with clients to ensure they are getting the most value from the system and to identify any opportunities for optimization or expansion.

6-Channels

1. **Direct Sales**

We engage with clients through a direct sales approach, offering personalized consultations, product demonstrations, and tailored proposals. Our sales team actively reaches out to potential clients and works closely with them to understand their needs and offer the most suitable solution.

2. **Website and Online Platform**

Our website serves as a primary channel for providing information about our products, services, and latest developments. Clients can access product specifications, case studies, and testimonials. Additionally, the website features contact forms and chatbots to facilitate direct communication and immediate support.

3. **Customer Support Hotline**

We offer a dedicated customer support hotline for real-time assistance. Clients can contact our support team to resolve technical issues, request maintenance services, or get answers to any questions they may have about our solutions.

4. **Email Communication**

Email is a key communication channel for sharing important updates, providing ongoing support, and offering product information. Through email, we send newsletters, updates on system improvements, and customer-specific reports, ensuring continuous engagement.

5. **In-Person Meetings and Workshops**

For larger projects and partnerships, we conduct in-person meetings and workshops with clients. These face-to-face interactions allow for more in-depth discussions, demonstrations, and training sessions, ensuring a hands-on approach to problem-solving and system deployment.

6. **Partner Networks and Resellers**

We work with a network of partners and authorized resellers to expand our reach and offer localized support in different regions. These partners help in distribution, installation, and after-sales support, making our solutions accessible to a wider audience.

7. **Social Media**

Social media platforms such as LinkedIn and Twitter serve as additional channels for engaging with clients, sharing industry news, and promoting new products or services. These platforms allow for more casual, real-time interactions and help us stay connected with our client base.

8. **Customer Portal**

We provide a secure, client-specific online portal where customers can access their account information, system performance data, technical documentation, and support resources. This self-service platform enhances the client experience by offering instant access to valuable tools and information.

9. **Trade Shows and Industry Events**

We participate in trade shows, conferences, and industry-specific events to showcase our solutions and engage with potential clients. These events provide an excellent opportunity for direct interaction, networking, and building relationships with key industry players.

7-Key Partners

Our business relies on strategic partnerships to enhance innovation, expand our capabilities, and ensure the smooth operation of our processes. The key partners include:

1. Funding and Investment Partners

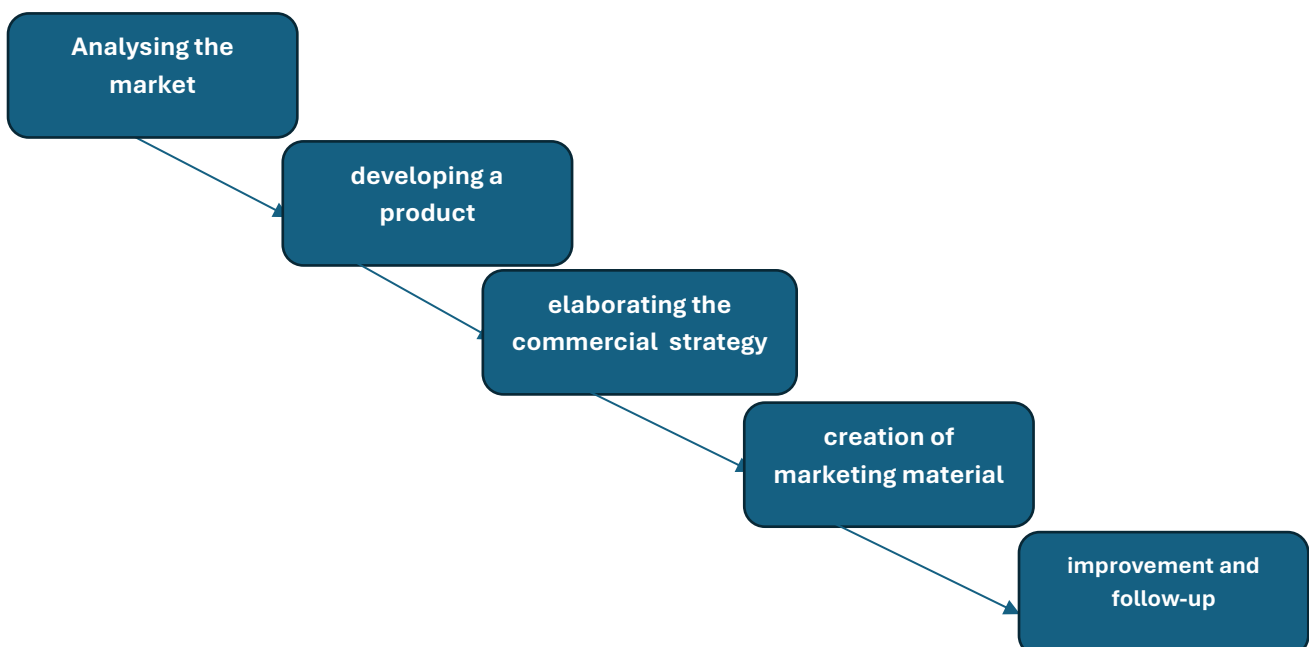
- **Algerian Startup Fund (ASF):**

ASF provides financial support and investment opportunities for startups in Algeria. This partnership helps us secure the necessary funding to develop and scale our air quality monitoring systems, enabling growth and long-term sustainability.

2. Main Suppliers

- **Raw material suppliers:**
- **Business equipment suppliers** (equipment used for our process)

8- Key Steps



7.1-Secondary Activities

In addition to our core focus on air quality monitoring systems, we engage in several secondary activities:

1. **Consultation Services**
Providing expert assessments and recommendations for air quality management.
2. **Research Collaboration**
Partnering with academic institutions on projects to advance air quality monitoring technologies.
3. **Community Engagement**
Promoting awareness of air pollution issues through local events and educational materials.
4. **Sustainability Initiatives**
Committing to environmental responsibility and supporting green practices.
5. **Technical Support**
Offering maintenance and technical assistance for existing monitoring systems.
6. **Data Analysis**
Providing insights and recommendations based on air quality data analysis.
7. **Networking Events**
Participating in industry conferences to connect with potential partners and clients.

7.2- Material Resources:

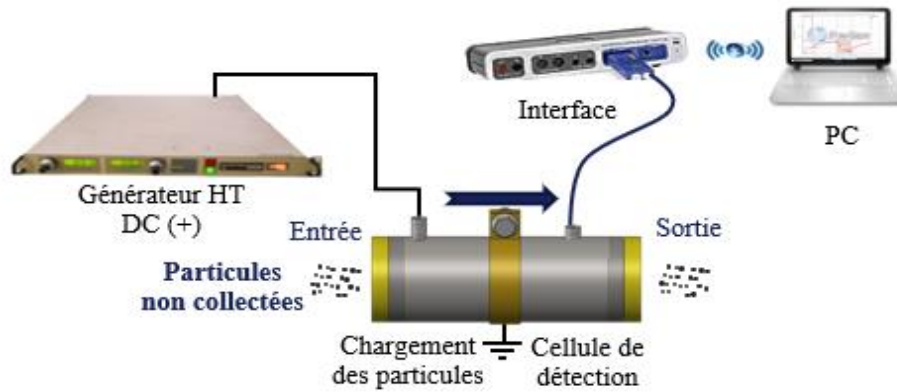


Figure 1: ECS prototype

8-Cost Structure

Cost Component	Amount (USD/DA)	Description
Research and Development (R&D)	64000DA	Continuous innovation, prototyping, testing, and refinement of sensors and software.
Raw Materials and Equipment	48000D	
- Raw Material Costs	26000DA	50 cm Tube Al Ø40mm 6000DA/m 50 cm tube Al Ø 60 mm 9000DA/m 50 cm Tube PTFE Ø 60 mm 14000DA/m 50 cm Tube PTFE Ø 80 mm 20000DA/m

		2 fiches BNC 200 DA raw martials 2000DA
- Equipment Costs	1300\$	interface Pasco 550 1100 \$ Charge sensor 160\$ High Voltage Generator 40 \$
Manufacturing and Production	12000DA	Labor, overhead, and production costs for sensor manufacturing and system assembly.
Installation and Maintenance	32000DA	
- Installation Costs	19200DA	Expenses related to deploying systems at client sites (labor, travel).
- Maintenance Costs	12800DA	Ongoing system maintenance, calibration, and technician support.
Sales and Marketing	32000DA	Marketing campaigns, client outreach, trade shows, and sales team expenses.
Administrative Costs	16000DA	Office expenses, utilities, salaries, legal, and accounting fees.
Training and Client Support	8000DA	Training materials, customer service, and ongoing client support.
Total	270000DA+1300\$	

Abstract (English)

Aerosols containing submicron particles suspended in the air, with diameters less than 1 μm , pose risks to health, the environment, air quality, and various industrial processes. Submicron particle detection systems measure the number or mass concentration of particles in the size range of 1 nm to 1 μm using techniques such as accumulated charge measurement (ELPI, SMPS) and optical measurement (Palas granulometer) for aerosols between 0.2 and 1 μm .

However, a significant drawback of these devices is their operational mode, which prevents continuous placement in filtration systems due to saturation and the risk of damage to optical components.

This study introduces a novel electrical detection system for the presence of particles within miniature aerosol sensors (compact and lightweight). The system measures the electric charge of particles induced by an electric field resulting from ion migration generated by a corona discharge charger. This method evaluates the total electric charge of flowing particles without requiring collection within the sensor. A sensitive electrometer is used to assess the collection efficiency of electrostatic precipitators.

Keywords: electric charge, corona discharge, Faraday cage, detection sensor.

Résumé—Les aérosols contenant des particules submicronique en suspension dans l'air et dont les diamètres sont inférieurs à 1 μm , sont néfastes pour la santé, l'environnement, la qualité de l'air ainsi que pour divers processus industriel. Les systèmes de détection des particules submicronique permettent de mesurer la concentration en nombre ou en masse des particules dans la plage de taille comprise entre 1 nm et 1 μm à l'aide d'une technique de mesure de charge accumulée sur les particules (ELPI, SMPS) et mesure optique (granulomètre Palas) pour les aérosols de 0.2 à 1 μm .

Cependant, le problème majeur de ces appareils est leur mode de fonctionnement, c'est-à-dire qu'ils ne peuvent pas être placés en continu dans des dispositifs de filtration, en raison de leur saturation et le risque de détérioration de leurs organes optiques.

Dans cette étude, un nouveau système de détection électrique de la présence de particules à l'intérieur de capteurs d'aérosols miniatures (compacts et légers) a été développé pour mesurer la charge électrique des particules induite par un champ électrique résultant de la migration des ions produits par un chargeur à effet couronne. Cette méthode repose sur la mesure de la charge électrique totale des particules en écoulement, sans nécessité de collecte à l'intérieur du capteur, à l'aide d'un électromètre sensible pour évaluer l'efficacité de collecte des électrofiltres.

Mot clés : charge électrique, décharge couronne, cage faraday, capteur de détection.

الملخص

تحتوي الهباء الجوي على جسيمات دقيقة أقل من 1 ميكرومتر معلقة في الهواء، والتي تشكل مخاطر على الصحة والبيئة وجودة الهواء والعديد من العمليات الصناعية. تقوم أنظمة الكشف عن الجسيمات الدقيقة بقياس تركيز العدد أو الكتلة (ELPI, SMPS) للجسيمات في نطاق حجم يتراوح بين 1 نانومتر و1 ميكرومتر باستخدام تقنيات قياس الشحنة المترجمة للجسيمات التي يتراوح حجمها بين 0.2 و1 ميكرومتر (Palas) والقياس البصري (مقياس الحبيبات).

ومع ذلك، فإن العيب الرئيسي لهذه الأجهزة هو طريقة عملها، حيث لا يمكن وضعها بشكل مستمر داخل أنظمة الترشيح بسبب التشبع وخطر تلف مكوناتها البصرية.

تقدم هذه الدراسة نظامًا جديدًا للكشف الكهربائي عن وجود الجسيمات داخل مستشعرات الهباء الجوي المصغرة (المضغوطة والخفيفة الوزن). يقيس النظام الشحنة الكهربائية للجسيمات الناتجة عن حقل كهربائي ينتج عن هجرة الأيونات المتولدة بواسطة جهاز شحن بتأثير الهالة (كورونا). تعتمد هذه الطريقة على قياس الشحنة الكهربائية الإجمالية للجسيمات المتدفقة دون الحاجة إلى جمعها داخل المستشعر، باستخدام مقياس كهربائي حساس لتقييم كفاءة الجمع للمرسبات الكهروستاتيكية.

الشحنة الكهربائية، تفريغ الهالة، قفص فاراداي، مستشعر الكشف: الكلمات المفتاحية.